AFFDL-TR-71-168

THE APPLICATION OF INVARIANT MODELING TO THE CALCULATION OF ATMOSPHERIC TURBULENCE

COLEMAN duP. DONALDSON
ROGER D. SULLIVAN

AERONAUTICAL RESEARCH ASSOCIATES OF PRINCETON, INC.

TECHNICAL REPORT AFFDL TR-71-168

JANUARY 1972

AIR FORCE FLIGHT DYNAMICS LABORATORY
AIR FORCE SYSTEMS COMMAND
WRIGHT-PATTERSON AIR FORCE BASE, OHIO

NOTICE

When Government drawings, specifications, or other data are used for any purpose other than in connection with a definitely related Government procurement operation, the United States Government thereby incurs no responsibility nor any obligation whatsoever; and the fact that the government may have formulated, furnished, or in any way supplied the said drawings, specifications, or other data, is not to be regarded by implication or otherwise as in any manner licensing the holder or any other person or corporation, or conveying any rights or permission to manufacture, use, or sell any patented invention that may in any way be related thereto.

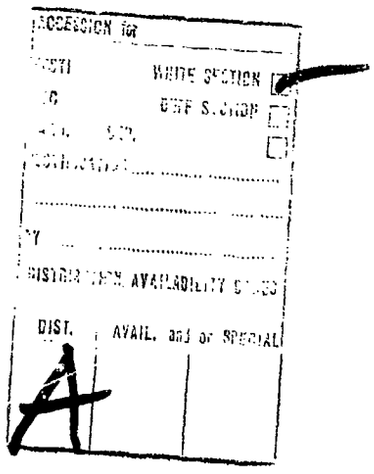

Copies of this report should not be returned unless return is required by security considerations, contractual obligations, or notice on a specific document.

AIR FORCE: 30-3-72/350

UNCLASSIFIED
Security Classification

DOCUMENT CONTROL DATA – R & D

(Security classification of title, body of abstract and indexing annotation must be entered when the overall report is classified)

1. ORIGINATING ACTIVITY *(Corporate author)*
Aeronautical Research Associates of Princeton, Inc.
50 Washington Road
Princeton, New Jersey 08540

2a. REPORT SECURITY CLASSIFICATION
U

2b. GROUP

3. REPORT TITLE
THE APPLICATION OF INVARIANT MODELING TO THE CALCULATION OF ATMOSPHERIC TURBULENCE

4. DESCRIPTIVE NOTES *(Type of report and inclusive dates)*
Final Report; 16 November 1970 - 15 October 1971

5. AUTHOR(S) *(First name, middle initial, last name)*
Coleman duP. Donaldson
Roger D. Sullivan

6. REPORT DATE	7a. TOTAL NO. OF PAGES	7b. NO. OF REFS
October 1971	65	27

8a. CONTRACT OR GRANT NO.	9a. ORIGINATOR'S REPORT NUMBER(S)
F33615-71-C-1051	A.R.A.P. Report No. 171
b. PROJECT NO. 682E	9b. OTHER REPORT NO(S) *(Any other numbers that may be assigned this report)* AFFDL TR-71-168
c.	
d.	

10. DISTRIBUTION STATEMENT
Approved for public release; distribution unlimited

11. SUPPLEMENTARY NOTES	12. SPONSORING MILITARY ACTIVITY
	Air Force Flight Dynamics Laboratory AFSC, Wright-Patterson Air Force Base, Ohio 45433

13. ABSTRACT

A method for the calculation of turbulent shear flows by an invariant modeling closure of the equations for the second-order correlations of fluctuating quantities in a turbulent medium is described. The relationship of the primary computational scale used in this model and the longitudinal integral scale of the turbulence under consideration is determined. With these results in hand, a technique is described by which it should be possible to determine the intensity and integral scale of turbulence measured by instrumented aircraft when only partial spectra are available. This is possible when the distributions of mean wind velocity and temperature in the atmosphere in the vicinity of the tests are available. Preliminary calculations using the method for a case when both the intensity and integral scale of turbulence were known yielded very good agreement between computed and experimental results.

DD FORM 1 NOV 68 1473

Unclassified
Security Classification

14. KEY WORDS	LINK A ROLE	LINK A WT	LINK B ROLE	LINK B WT	LINK C ROLE	LINK C WT
Turbulence						
Invariant Modeling						
Turbulent Shear Flow						
Free Jet						
Free Shear Layer						
Boundary Layer						

☆U.S.Government Printing Office: 1972 — 759-084/456

FOREWORD

This report was prepared by the Aeronautical Research Associates of Princeton, Inc., Princeton, New Jersey, under Contract Number F33615-71-C-1051, Project Number 682E. The principal investigator was Dr. Coleman duP. Donaldson; the research covers the period from 16 November 1970 through 15 October 1971. The contractor's report number is A.R.A.P. 171.

It is the authors' duty and pleasure to acknowledge here the help they have received in preparing this report from their colleagues at A.R.A.P. and from those at the Flight Dynamics Laboratory who have concerned themselves with this study. Special thanks are due to Dr. John Houbolt at A.R.A.P. and Dr. Peter Conrad, a former associate at A.R.A.P., for their interest and helpful discussions. Our thanks are also due to Messrs. Paul Hasty and Jan Garrison of the Flight Dynamics Laboratory for their help in selecting, out of a vast number of flight measurements of atmospheric turbulence, those most suitable for consideration in this study.

This technical report has been reviewed and is approved.

GORDON R. NEGAARD, Major, USAF
Chief, Design Criteria Branch
Structures Division

ABSTRACT

A method for the calculation of turbulent shear flows by an invariant modeling closure of the equations for the second-order correlations of fluctuating quantities in a turbulent medium is described. The relationship of the primary computational scale used in this model and the longitudinal integral scale of the turbulence under consideration is determined. With these results in hand, a technique is described by which it should be possible to determine the intensity and integral scale of turbulence measured by instrumented aircraft when only partial spectra are available. This is possible when the distributions of mean wind velocity and temperature in the atmosphere in the vicinity of the tests are available. Preliminary calculations using the method for a case when both the intensity and integral scale of turbulence were known yielded very good agreement between computed and experimental results.

TABLE OF CONTENTS

LIST OF ILLUSTRATIONS

I. INTRODUCTION

Some time ago, the senior author of this paper proposed an approach to the computation of turbulent shear flows (Ref. 1) which, because of its generality, gave promise of allowing one to make calculations of turbulent atmospheric and vortex motions. In 1969 this method in its earliest form, was applied to the calculation of the generation of turbulence in the atmosphere (Ref. 2). The results of these calculations were intriguing enough to warrant refinement of the method and its further application to calculations of the generation of atmospheric turbulence. During fiscal year 1971 support was obtained from two sources towards these two ends. A moderate level of support was obtained from NASA under Contract No. NASW-1868 for further refinement of the method and a somewhat higher level of support was obtained from the Air Force for development of the method for application to a specific problem faced by the Flight Dynamics Laboratory; this report discusses the results obtained for the Air Force.

II. STATEMENT OF THE PROBLEM

A problem that has faced and continues to face the Flight Dynamics Laboratory's Design Criteria Branch is that of determining two fundamental characteristics of atmospheric turbulence under any given set of conditions. These characteristics or parameters, which define in a gross way the structural response of aircraft to atmospheric turbulence, are the root mean square of the vertical component of the turbulent velocity field σ_w and an integral scale of the turbulent velocity field L. In general, it is assumed, for work concerned with structural problems, that the turbulent velocity field is sufficiently isotropic so that only two integral scales must be considered. One is the longitudinal integral scale L defined by

$$L = L_{11} = \frac{1}{\langle u_1' u_1' \rangle (\underline{x})} \int_o^\infty \langle u_1'(\underline{x}) u_1(\underline{x} + x_1) \rangle dx_1 \qquad (1)$$

The other is the transverse integral scale L_{33}

$$L_{33} = \frac{1}{\langle u_3' u_3' \rangle (\underline{x})} \int_o^\infty \langle u_3'(\underline{x}) u_3'(\underline{x} + x_1) \rangle dx_1 = L_{22} \qquad (2)$$

It is well-known from the theory of isotropic turbulence (Ref. 3) that these scales are related; namely,

$$L = L_{11} = 2L_{33} = 2L_{22} \qquad (3)$$

For the calculations involved in practical structural design, it has been assumed that Eq. (3) is valid, so that the problem facing the structural designer is that of determining σ_w and L for any given atmospheric situation.

In principle, the determination of these two parameters is straightforward. In practice, however, the task is impossible in many cases because accurate measurements of turbulence intensity are not available over a wide enough range of wave numbers. Consider the spectrum of turbulence shown in Figure 1. This spectrum, taken from Ref. 4, represents the power spectral density $\Phi_w(\Omega)$ of the turbulent vertical velocity w' measured in a thunderstorm, plotted against the reduced frequency Ω. This spectrum is typical of many atmospheric spectra that have been obtained. The trustworthy portion of the spectrum exhibits a $\Phi_w \sim \Omega^{-5/3}$ behavior throughout. This behavior, while it is gratifying to students of turbulent motions, does not permit one

to estimate either the integral scale or the intensity of the turbulence. It has been pointed out by Houbolt that, if the actual spectrum is a von Karman spectrum, namely,

$$\Phi_w = \frac{\sigma_w^2 L}{\pi} \frac{1 + \frac{8}{3}(1.339L\Omega)^2}{[1 + (1.339L\Omega)^2]^{11/6}} \qquad (4)$$

one can infer from a record such as that shown in Figure 1 only the following relationship between the intensity and the integral scale:

$$\sigma_w^2 = \frac{1}{0.521} \Omega^{*5/3} \Phi_w^* L^{2/3} \qquad (5)$$

where Ω^*, Φ_w^* represents any point on the minus five-thirds slope portion of the spectrum. Two spectra satisfying Eq. (4) are shown in Figure 1. One spectrum is for $\sigma_w = 32.33$ ft/sec and $L = 5600$ feet, while the second is for $\sigma_w = 25.66$ ft/sec and $L = 2800$ feet.

This example illustrates the difficulty of finding the quantities σ_w and L when only partial spectra, such as the one just discussed, are given. The study supported under the present contract was an effort to develop a method by which it might be possible to estimate both σ_w and L from partial spectra when the profiles of mean wind and atmospheric temperature were available.

The technique proposed was the following. The method of invariant modeling permits, as is shown below, the computation of the turbulent structure of the atmosphere if the local mean wind and temperature profiles are known. This computation is possible if a scale parameter Λ_1, related to L, is assumed. The relationship between computed σ_w and assumed L is different than that given in Eq. (5). Thus, if the relationship of L and Λ_1 is known, it is possible to determine both L_{11} and σ_w by finding the intersection of the curve representing Eq. (5) and of the curve obtained from the results of the computations.

The study undertaken for the Air Force consisted of two parts. First, detailed investigations were carried out in which computations of turbulence in a free shear layer and in an axially symmetric free jet were made. In these studies, the local value of Λ_1 was found in each case that best reproduced, within the ability of the mathematical model, the turbulent structure of the particular flow under investigation. This was possible because of the fairly large amount of detailed information concerning the turbulent structure of these two flows. The local value of Λ_1

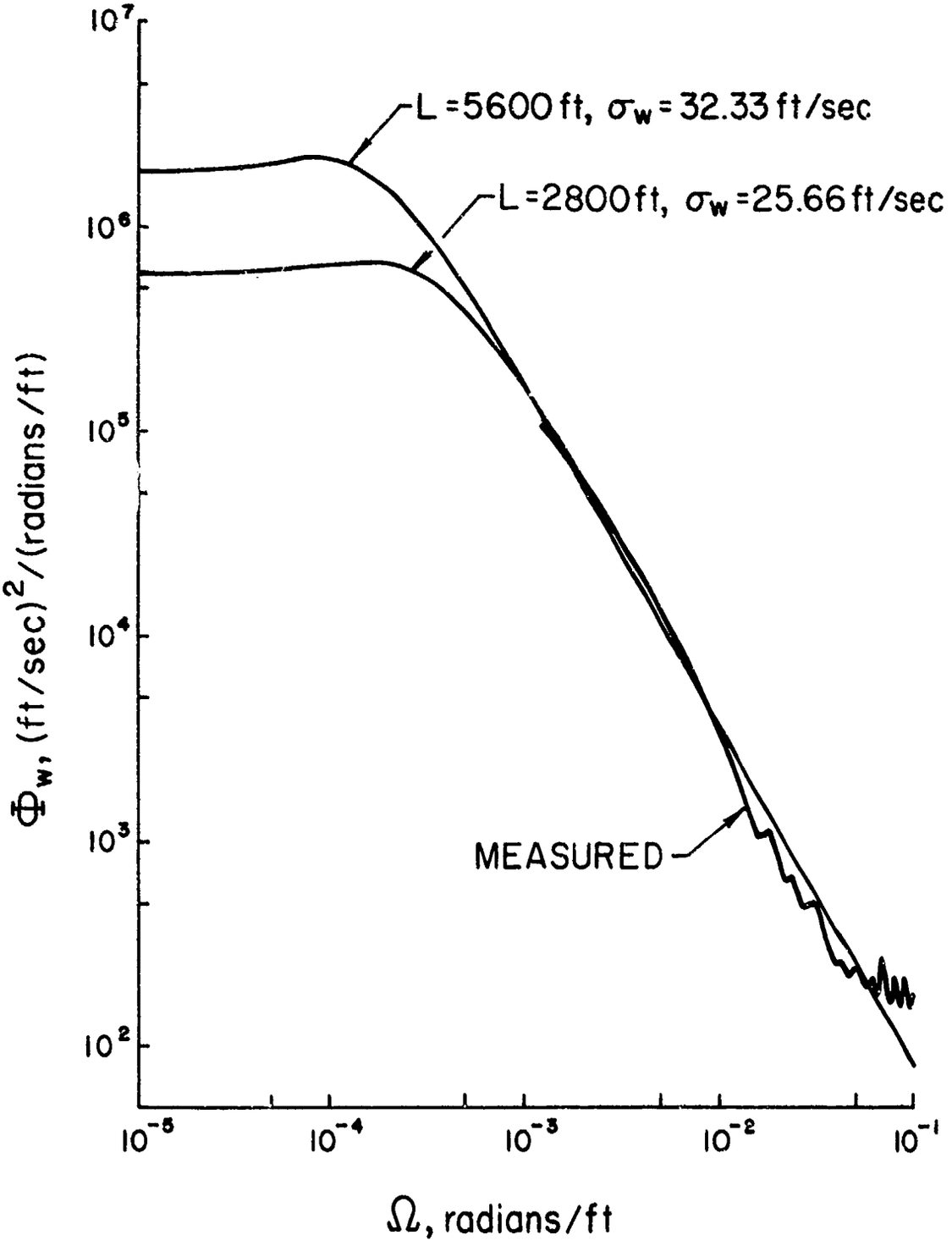

Fig. 1. Power spectrum measured in a thunderstorm (Ref. 4) and two von Kármán spectra fitted to it

was then compared with the local value of L as measured in each case. In this way, it was determined that the following relationship between L and Λ_1 is representative:

$$\Lambda_1 \simeq 0.6L$$

Second, with this result in hand, a computation was carried out, as an initial test case, to see if the method discussed above for recovering atmospheric scales and intensities was plausible.

III. DESCRIPTION OF AN INVARIANT MODEL OF TURBULENT SHEAR LAYERS

The equation for the time-independent mean velocity in an incompressible turbulent medium was given many years ago by Reynolds (Ref. 5). It is

$$\rho\bar{u}^j\bar{u}_{i,j} = -\bar{p}_{,i} + \left(\bar{\tau}_i^j - \rho\langle u^{j\prime}u_i'\rangle\right)_{,j} \tag{6}$$

In this paper, bars over a quantity or angular brackets around a quantity indicate average values of that quantity while primes indicate the instantaneous fluctuation of the quantity from its mean value. The mean molecular stress $\bar{\tau}_i^j$ is given by

$$\bar{\tau}_i^j = g^{jk}\mu\left(\bar{u}_{i,k} + \bar{u}_{k,i}\right) \tag{7}$$

The second-order correlation of the velocity fluctuations that appears in Eq. (6) represents the transport of momentum by turbulent eddies and is called the Reynolds stress. An equation for this second-order tensor was also given by Reynolds. It is, for steady flow,

$$\begin{aligned}\rho\bar{u}^j\langle u_i'u_k'\rangle_{,j} = {} & -\rho\langle u^{j\prime}u_k'\rangle\bar{u}_{i,j} - \rho\langle u^{j\prime}u_i'\rangle\bar{u}_{k,j} - \rho\langle u^{j\prime}u_i'u_k'\rangle_{,j} \\ & - \langle u_i'p'\rangle_{,k} - \langle u_k'p'\rangle_{,i} + \langle p'(u_{i,k}' + u_{k,i}')\rangle \\ & + \mu g^{mn}\langle u_i'u_k'\rangle_{,mn} - 2\mu g^{mn}\langle u_{i,m}'u_{k,n}'\rangle\end{aligned} \tag{8}$$

In the past, it has been customary to carry out investigations of turbulent shear flows by means of Eq. (6). In these studies the unknown second-order velocity correlation term was modeled in terms of the mean velocity and a length. Computations made in this manner form the vast bulk of the literature on turbulent shear flow calculations to the present time. The methods that are now in use employing this type of modeling, having evolved over a period of many years, are exceedingly useful and enough empirical data have been amassed to enable one to calculate solutions to a wide variety of engineering problems with a great deal of confidence. There are, however, a number of problems facing engineers today which require the calculation of turbulent shear flows for which there is no existing body of experimental data. Two flows which come readily to mind are the generation of turbulence and turbulent transport correlations by the earth's atmosphere and the decay of a turbulent vortex. In the case of these two flows, we may ask ourselves the following questions: "Is there not a somewhat more basic method of computing turbulent transport phenomena than the

eddy viscosity or mixing length models presently in use?" "Can not such a method permit us to generalize the experimental results that presently exist so as to estimate the nature of turbulent flows that have not yet been investigated experimentally?" The answers to these two questions are not as straightforward as one would like. In answer to the question as to whether there is a more basic method, the reply must be: Yes, but the real difficulty comes when one tries to establish just how much more fundamental the proposed new method is to be. If a new method is truly more fundamental, then it will allow better estimates of unknown flows than can be made by older techniques. It is fair to say, at the present time, that there is considerable hope among those who practice the art of calculating turbulent shear flows that the new methods now being developed, of which the method to be described here is but one, take into account enough physics that is not contained in older models so that a technological advance can be made. It is as yet too early in the history of these new methods to make any strong statement as to just how much more powerful they are than the older methods.

If one wishes to make use of both Eqs. (6) and (8) in computing turbulent shear flows, the first step must be a choice of models for those terms in Eq. (8) which are not expressed in terms of the mean velocity or the second-order velocity correlation. The terms which must be modeled are

(1) the pressure-strain correlation in the tendency-towards-isotropy term, namely, $\langle p'(u'_{i,k} + u'_{k,i})\rangle$;

(2) the third-order tensor in the velocity diffusion term, namely, $\langle u'_i u'_j u'_k\rangle$;

(3) the pressure velocity correlation in the pressure diffusion terms, namely, $\langle u'_i p'\rangle$;

(4) the general viscous dissipation term $2\mu g^{mn}\langle u'_{i,m} u'_{k,n}\rangle$

There are many ways in which a modeling of the above-noted terms may be accomplished. We have tried, for our initial investigation, to take as simple a model as possible for each term. We have then attempted to determine by calculation the adequacy of the chosen model and the sensitivity of the calculated results to the particular choice of model.

To date the following models have been investigated to some extent.

(1) For the tendency-towards-isotropy term, we choose, following Rotta (Ref. 6), the following model:

$$\langle p'(u'_{i,k} + u'_{k,i})\rangle = -\frac{\rho q}{\Lambda_1}\left(\langle u'_j u'_k\rangle - g_{ik}\frac{K}{3}\right) \qquad (9)$$

where

$$q^2 = K = \langle u^{m'} u'_m \rangle = \langle u'^2 \rangle + \langle v'^2 \rangle + \langle w'^2 \rangle \tag{10}$$

and Λ_1 is a scalar length associated with the tendency towards isotropy and is to be identified. More complicated models of this term have been discussed by Chou (Ref. 7) and by Hanjalic and Launder (Ref. 8). To date, we have had considerable success using the simple Rotta model given above and, in line with our philosophy of using the simplest possible model that will give reliable results, we have confined the majority of our computational studies to the use of Eq (9).

(2) For the velocity diffusion term, we must model $\langle u'_i u'_j u'_k \rangle$. The simplest covariant tensor of rank three that is symmetric in all three indices that we can form out of the second-order correlations is

$$\langle u'_i u'_j \rangle_{,k} + \langle u'_j u'_k \rangle_{,i} + \langle u'_k u'_i \rangle_{,j}$$

This expression has all the tensor and symmetry characteristics required of our model. To make it dimensionally correct, the above expression must be multiplied by a scalar velocity and a scalar length. The simplest scalar velocity we can form from the second-order correlations is $\sqrt{\langle u^{m'} u'_m \rangle} = q$, so we model the tensor $\langle u'_i u'_j u'_k \rangle$ as

$$\langle u'_i u'_j u'_k \rangle = -\Lambda_2 q \left[\langle u'_i u'_j \rangle_{,k} + \langle u'_j u'_k \rangle_{,i} + \langle u'_k u'_i \rangle_{,j} \right] \tag{11}$$

where Λ_2 is a scalar length associated with velocity diffusion and is also to be identified by matching experimental results.

(3) The pressure velocity correlation $\langle p' u'_k \rangle$ in the pressure diffusion term is modeled by analogy with the velocity diffusion term as

$$\langle p' u'_k \rangle = -\rho \Lambda_3 q \langle u^{m'} u'_k \rangle_{,m} \tag{12}$$

In our work, in order to cut down the number of parameters in our turbulence model, we have considered only two special cases of Eq. (12). We have considered the case $\Lambda_3 = \Lambda_2$ and the case where $\langle p' u'_k \rangle = 0$, i.e., the case $\Lambda_3 = 0$.

(4) We have considered two models for the expression $g^{mn} \langle u'_{i,m} u'_{k,n} \rangle$ appearing in the viscous dissipation term:

(a) $$g^{mn} \langle u'_{i,m} u'_{k,n} \rangle = \frac{\langle u'_i u'_k \rangle}{\lambda^2} \tag{13}$$

and

$$\text{(b)} \qquad g^{mn}\langle u'_{i,m}u'_{k,n}\rangle = \frac{K}{3\lambda^2} \tag{14}$$

In both these models, λ is a dissipative length scale. The argument for choosing the latter expression is that it is expected that the turbulence will be almost isotropic in that part of the spectrum responsible for dissipation of turbulent kinetic energy. Thus, one would expect the dissipation to be almost isotropic even if the turbulence itself is not. Further, there is experimental evidence that the loss of shear correlation by viscous action is relatively much smaller than the loss of kinetic energy by viscous action. In our initial computations using Eq. (14) as a model of dissipation, we experienced some difficulties in obtaining solutions. There was a tendency for solutions to develop with negative values for the mean square velocities when the turbulence became very nonisotropic. This tendency was overcome by the use of Eq. (13) for the dissipation model. This model does not have a large effect on the development of the shear correlations because the primary contribution to loss of shear with this model is not the dissipation term but the tendency-towards-isotropy term. Although the whole question of modeling the dissipation term is still under investigation, the work reported here was carried out using Eq. (13), for the reasons stated above.

In the models given above, we would expect that the scalar lengths Λ_1, Λ_2, and Λ_3 would all be related to the local integral scale of the turbulence. These lengths are, in turn, related to the local scale of the mean motion for the flows we shall investigate here, and we make the assumption in the computations we will discuss presently that Λ_1, Λ_2, and Λ_3 are all proportional to some local characteristic length δ_{char} of the mean motion under consideration.

We will expect the length appearing in the dissipation model to be related to the microscale of the turbulence which, in turn, must be related to the integral scale via a Reynolds number in such a way that production of turbulence is balanced to a large extent by dissipation.

If the models we have just discussed [Eqs. (9) and (11)-(13)] are substituted in the basic equation for the second-order velocity correlations [Eq. (8)], the resulting equation, taken together with the momentum and continuity equations, makes a closed set (see Appendix A). When this set is reduced to boundary layer form, it is found to form a parabolic system (see Appendix B).

This set of equations will admit similarity solutions at high Reynolds numbers as well as permit calculations of turbulent flows near walls, if one makes the following choice of the relation between the length scales:

$$\Lambda_1 = c_1 \delta_{char} \tag{15}$$

$$\Lambda_2 = c_2 \Lambda_1 = c_2' \delta_{char} \tag{16}$$

$$\Lambda_3 = c_3 \Lambda_1 = c_3' \delta_{char} \tag{17}$$

and

where

$$\lambda = \Lambda_1 / \sqrt{a + b \cdot Re_{\Lambda_1}} \tag{18}$$

$$Re_{\Lambda_1} = \rho q \Lambda_1 / \mu \tag{19}$$

For self-similar free turbulent flows, the structure given above is all that is needed to compute a turbulent shear layer or a free jet, provided the five constants, c_1, c_2, c_3, a, and b are given. To find these constants, we must resort to the comparison of calculated flow fields with experimental results.

If we wish to compute a boundary layer flow, we must consider an additional problem. When a wall is present in a shear flow, we wish to apply the boundary condition at the wall that

$$\langle u_i' u_k' \rangle_{z=o} = 0$$

where z is measured normal to the surface. In addition, there should be no diffusion of $\langle u_i' u_k' \rangle$ through the surface, so that $\partial \langle u_i' u_k' \rangle / \partial z = 0$ at $z = 0$. Thus, it is reasonable to assume that near the wall

$$\langle u_i' u_k' \rangle = A_{ik} z^{1+\eta} \tag{20}$$

where A_{ik} is a constant and η is a positive constant. But if there is no diffusion through the wall, then all that is diffused towards the wall by viscosity at $z = \epsilon$ is dissipated in the region between $z = \epsilon$ and $z = 0$. (It is easily verified that all other terms in the model equation for $\langle u_i' u_k' \rangle$ are neglible if ϵ is small enough.) Thus,

$$2\mu \int_o^{\epsilon} \frac{\langle u_i' u_k' \rangle}{\lambda^2} \, dz = \mu \left(\frac{\partial \langle u_i' u_k' \rangle}{\partial z} \right)_{z=\epsilon}$$

or, using Eq. (20)

$$2\int_0^{\epsilon} \frac{z^{1+\eta}}{\lambda^2} dz = (1 + \eta)\epsilon^{\eta}$$

If this relation is to hold for all $\epsilon \to 0$, we must have

$$\lambda = \alpha z \tag{21}$$

where

$$\alpha^2 = \frac{2}{(1 + \eta)\eta}$$

Thus, near a solid surface, we will always assume, in applying our model, that Eq. (21) holds in the region near the wall.

It is convenient to express this result in terms of Λ_1. Near a wall, Eq. (18) becomes

$$\lambda = \Lambda_1/\sqrt{a} \tag{22}$$

Using Eq. (21), we may write

$$\Lambda_1 = \alpha\sqrt{a}\, z \tag{23}$$

Thus, for boundary layer flows, α is another number which must be found from experimental results.

In our first attempts to construct a model of turbulent shear flows (Refs. 9 and 10), the following assumptions were made to construct the simplest possible model of boundary layer flows:

(1) It was assumed that all the large lambdas associated with inviscid modeling were equal, i.e., $\Lambda_1 = \Lambda_2 = \Lambda_3 = \Lambda$.

(2) It was assumed that α was equal to one.

(3) In the outer portion of a boundary layer, Λ was taken to be a constant c_1 times $\delta_{.99}$ ($\delta_{.99}$ is the value of z for which $\bar{u}$ is 99% of the free stream velocity). This value was assumed to hold, independent of z, as the wall was approached, until Λ became equal to $\sqrt{a}$ times z. For smaller values of z, Λ was taken equal to $\sqrt{a}\, z$.

With these assumptions, the boundary layer forms of Eqs. (6) and (8) with appropriate modeling (Appendix B) were solved with various choices for the parameters a, b, and $c_1 = \Lambda/\delta_{.99}$ to produce a developing turbulent boundary layer on a flat plate.

It was determined at that time that the following choice of parameters

$$c_1 = \Lambda/\delta_{.99} = 0.064$$
$$a = 2.5 \qquad (24)$$
$$b = 0.125$$

yielded a fair representation of a turbulent boundary layer. The mean velocity profile and the behavior of skin friction with Reynolds number were adequately represented. The distributions of the second-order correlations within the boundary layer were reasonable.

The results of this original parameter search were used to compute a number of other turbulent flows in order to demonstrate the method (Refs. 9 and 10).

Before proceeding with further applications, it was considered necessary that a more detailed parameter search should be made. In particular, two free turbulent flows - the free jet and the free shear layer - should be calculated to determine the values of the parameters c_2 , c_3 , a , and b that would best fit the experimental results for both flows. (The equations for the free shear layer are the same as those for the boundary layer given in Appendix B. The equations for the axially symmetric free jet are given in Appendix C.) The value of c_1 being the ratio of Λ_1 to some arbitrarily defined characteristic length in each case is not an invariant of the problem and was to be chosen, with fixed values of the other parameters, to obtain best results in each case. Once these studies were complete, the model would be used to compute turbulent boundary layer flows so that, by comparison with experimental results, values for c_1 and α could be made for this flow. Hopefully, all flows could be described in a reasonable way by a single choice of the basic model parameters c_2 , c_3 , a , b , and (where appropriate) α. The values of local Λ_1^3 determined from the values of c_1 in each case were then to be compared with the local magnitude of the integral scale L in each case. If it was found that the value of c_1 represented a choice that amounted to

$$\Lambda = \text{const } L = \beta L \qquad (25)$$

then it would be assumed that a reasonably invariant model had been determined.

IV. THE SEARCH FOR NEW MODEL PARAMETERS

Our search for a new model of turbulent shear layers began with an attempt to describe the axially symmetric free jet with the original turbulence model obtained for a boundary layer flow. This model, as mentioned in the previous section, was one for which $\Lambda_1 = \Lambda_2 = \Lambda_3 = \Lambda$. This choice leaves three parameters to be determined. They are $c_1 = \Lambda/\delta_{char}$ and the two constants a and b in the expression

$$\lambda = \Lambda/\sqrt{a + b \cdot Re_\Lambda}$$

The method of searching for values for these parameters was as follows. The equations for a free jet were programmed so as to solve the system of equations for a free jet developing in the axial direction. At an arbitrary initial station in the axial direction, a mean velocity profile and profiles of the pertinent second-order correlations were arbitrarily assumed. For a given choice of model parameters (in this case, a, b, and $c_1 = \Lambda/r_{.5}$, where $r_{.5}$ is the radius for which $\bar{u}$ is one-half the centerline value), the free jet equations were solved for the development of the jet downstream of the initial distributions. In all cases, essentially self-similar solutions were obtained far downstream of the start of the calculation. If a set of parameters could be found so that the resulting self-similar flow agreed with experimental measurements with respect to the rate of spread, as well as with respect to mean velocity and correlation distributions, it would then be assumed that a reasonable turbulence model had been achieved.

Actually, such calculations were carried out for both free jets and two-dimensional free shear layers. With the single Λ model, it was found that no combination of parameters a, b, and c_1 could produce an adequate description of either a free jet or a free shear layer. In general, it was found that if the parameters were adjusted so as to give an adequate rate of spread of the mean profile (i.e., if the level of the turbulent shear correlation was large enough) the spread of the correlations $\langle u_i' u_k' \rangle$ by diffusion was always too large. This general result is illustrated in Figure 2 where it is seen that, if the general level of the shear correlation $\langle u'w' \rangle$ were to match the experimental data of Wygnanski and Fiedler (Ref. 11) in the region of maximum shear, it is clear that far too long a tail of $\langle u'w' \rangle$ at large r would result. This was a very general result for free shear flows and forces us to consider a more complicated model.

The difficulty that was experienced with the constant model was the existence of too much diffusion relative to the rate of loss of correlations, either by dissipation or the tendency towards isotropy. To correct this difficulty in the studies

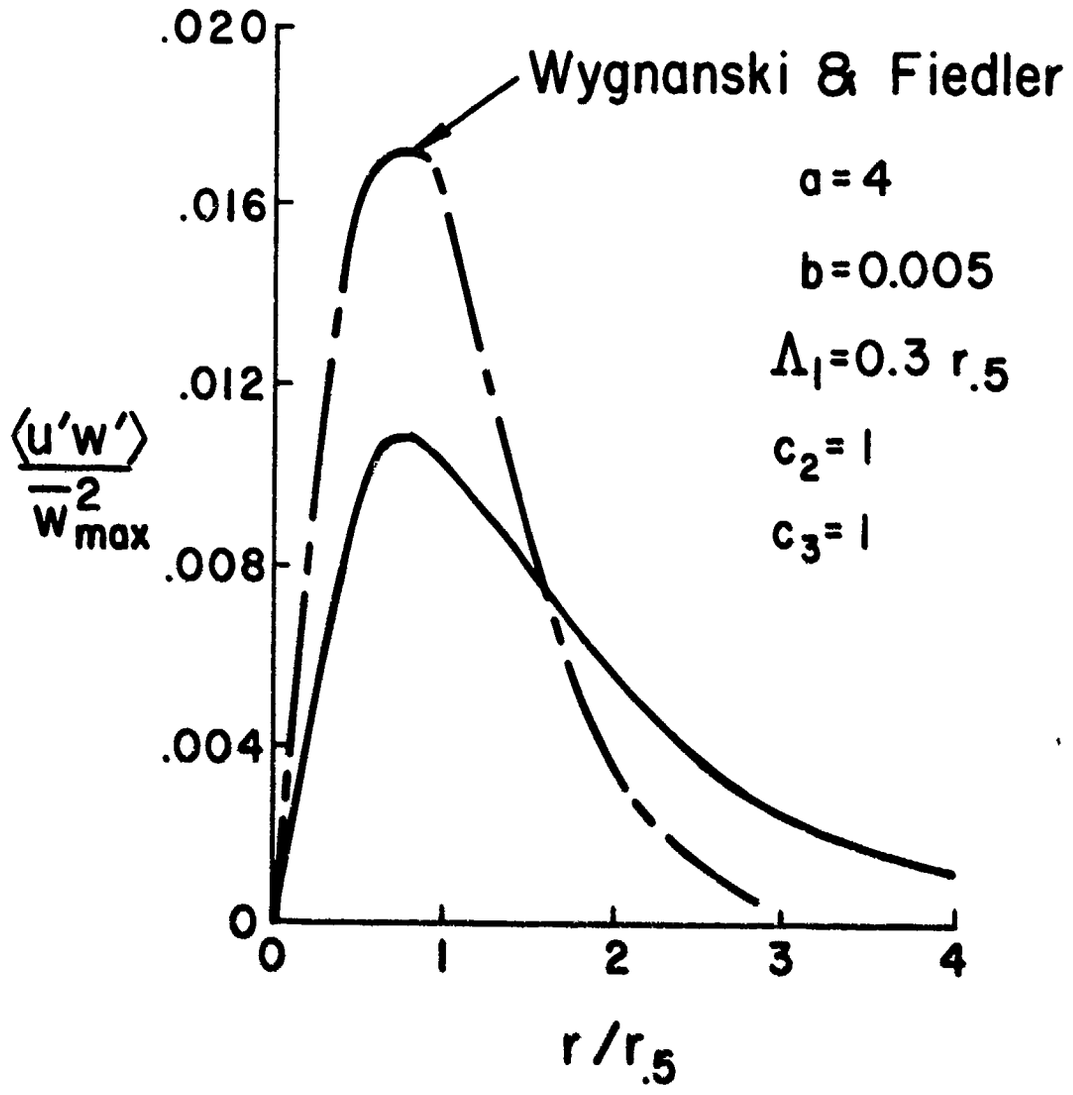

Fig. 2. Result of a free jet computation with a single Λ model of turbulence

reported here, the diffusion lengths Λ_2 and Λ_3 were made smaller than Λ_1. An idea of the effect of reducing the diffusion lengths relative to the isotropy length can be seen from Figure 3. Here the rms value of the longitudinal velocity fluctuation w', that has been calculated for several choices of model parameters, is plotted versus radius in a self-similar free jet. Note that as the diffusion lengths Λ_2 and Λ_3 (which are c_2 times Λ_1) are reduced, the amount of diffusion is obviously reduced and the levels of turbulence on the jet centerline are appreciably increased.

The effect of the choice of the scale of the isotropy length Λ_1 can be seen from Figure 4. The distribution of longitudinal turbulence intensity is shown as a function of radius for two choices of Λ_1 relative to the local value of $r_{.5}$. It is seen that the levels are much lower for the smaller Λ_1 than for the larger value. This is what one might expect because of the increased dissipation, as well as the increased loss of shear correlation by the tendency towards isotropy when the scale Λ_1 and, hence, λ is made smaller.

The effect of neglecting pressure diffusion can be seen in Figure 5; the longitudinal velocity fluctuations in a free jet are shown as a function of radial position for a given choice of model parameters a, b, c_1, and c_2 for two choices of c_3. One choice is $c_3 = c_2$ and the second is $c_3 = 0$, i.e., neglect of pressure diffusion. It is seen that for this choice of the other parameters, the effect of neglecting pressure diffusion is not large.

Having given some idea of how some of the various parameters entering the model for turbulent shear layers affect the solutions, we must now discuss the selection of an actual set of parameters. If one considers only a single type of shear flow that one wishes to model, say, the free jet, it is possible to choose a whole spectrum of models which will give a good description of the mean spread of the free jet and the distribution of, say, the longitudinal turbulent velocity field. To illustrate this point, we may refer to Figure 6. Here we see that two profiles of longitudinal velocity fluctuation can be obtained with radically different choices of b and Λ_1. It is observed that if one chooses small b one must also choose a small value of Λ_1 relative to a characteristic scale of the jet. What then is the basic difference between these two solutions? It is this. For the solution with small b and small Λ_1, the balance of the production of turbulence is more by dissipation and less by diffusion than for the other case. Also, for the case of small b and small Λ_1, the solutions are more isotropic on the jet centerline than for the other case.

The choice between the two models exhibited in Figure 6 must be made on the basis of the degree of diffusion and the degree of isotropy desired in the calculated result. This is a difficult decision to make, for existing experimental data do not agree as to how isotropic free jets are on their centerlines, as will be seen presently. There is another way that one can decide between

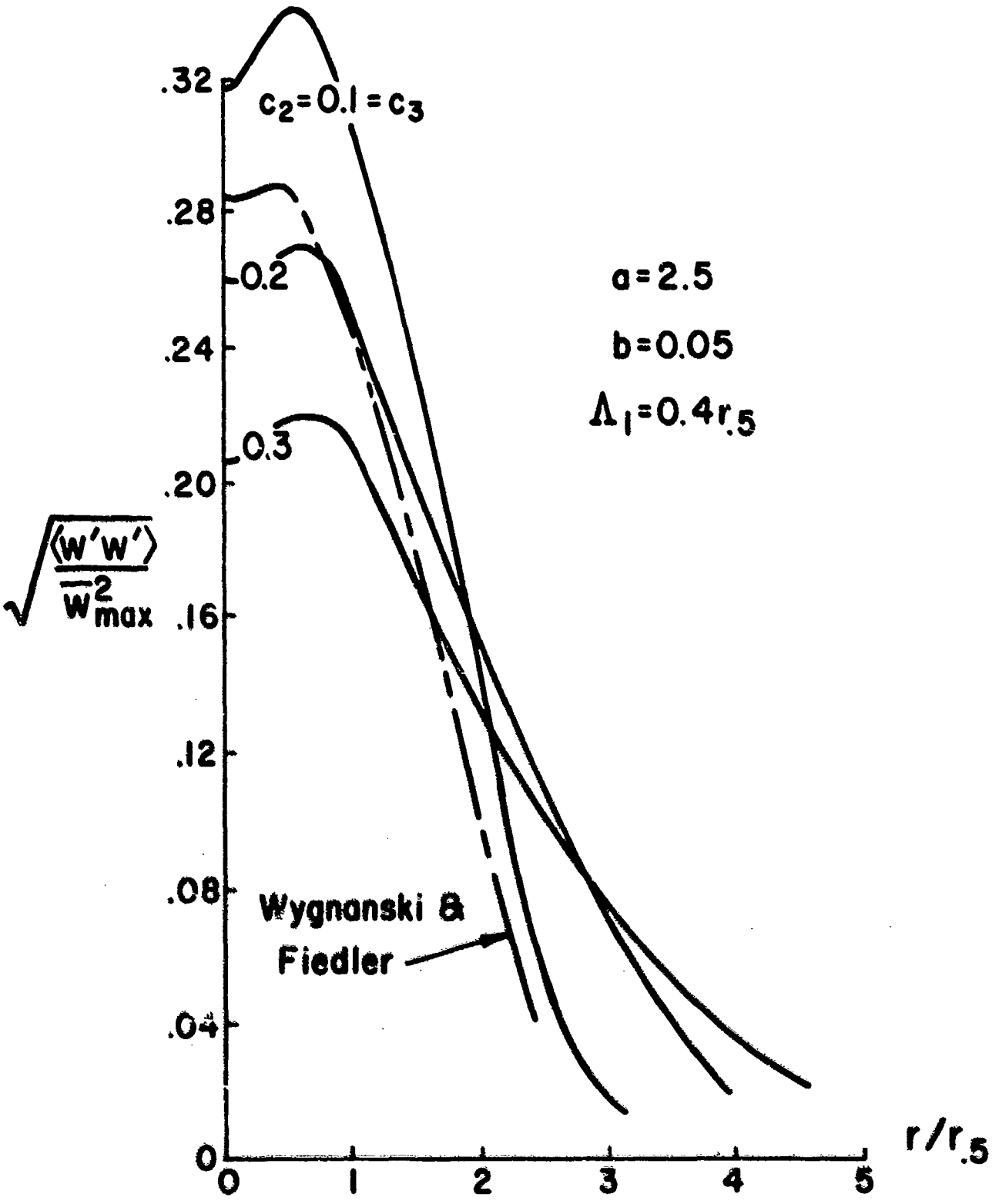

Fig. 3. Behavior of solutions for a self-similar free jet when the parameter $c_2 = \Lambda_2/\Lambda_1 = \Lambda_3/\Lambda_1$ is varied

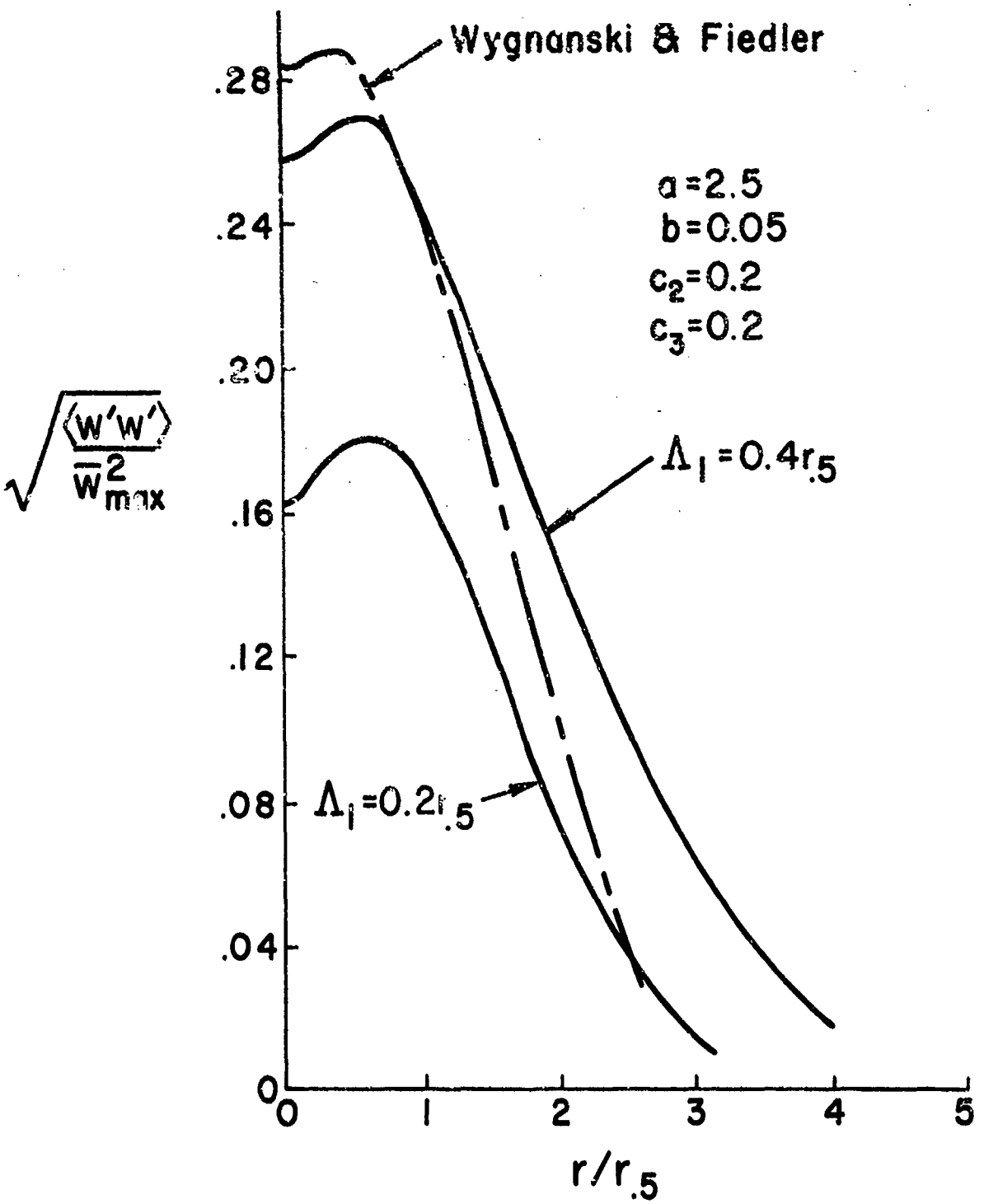

Fig. 4. Effect of variation of the isotropy scale Λ_1 on characteristics of a self-similar free jet

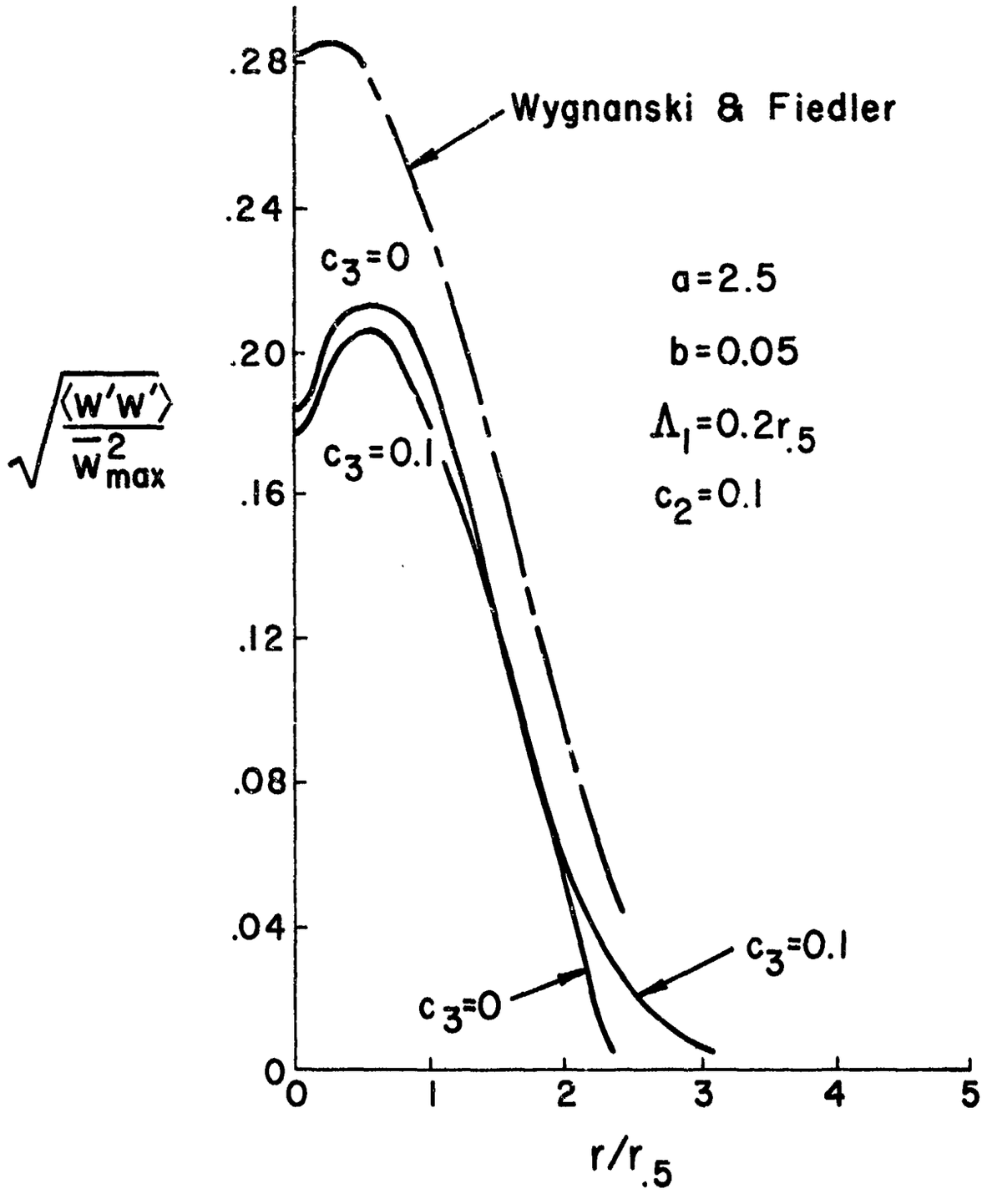

Fig. 5. The effect of neglecting pressure diffusion when calculating a self-similar free jet

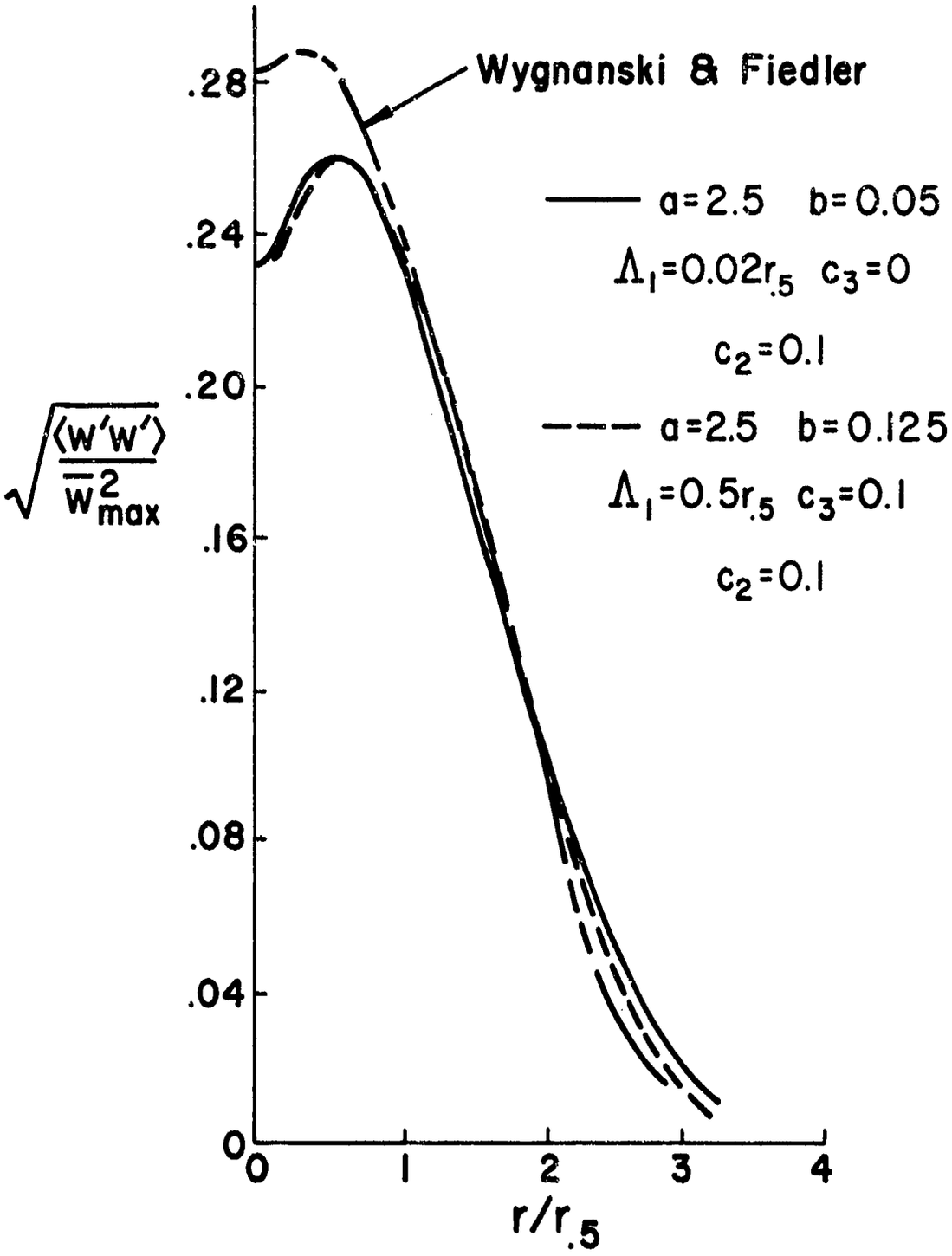

Fig. 6. Two choices of model parameters that yield almost the same distributions of $\langle w'w' \rangle$ for a self-similar free jet

two different models. If one uses the same model to compute two different turbulent flows having essentially different geometries, the model which gives the best results for both flows is, since we are seeking an invariant model, the one to choose.

As mentioned previously, we have computed self-similar solutions for a free shear layer as well as for an axially symmetric free jet. Actually a search for model parameters for each type of flow was carried out. As a result of these studies, it was determined that, insofar as the parameter studies have proceeded at this point, the following model for free turbulent shear flows gave the best results:

$$\begin{aligned} a &= 2.5 \\ b &= 0.125 \\ c_2 &= 0.10 \\ c_3 &= 0.10 \end{aligned} \tag{26}$$

Also, the value

$$c_1 = \Lambda_1/\delta_{char} = 0.50 \tag{27}$$

was found best for both flows, although it was not part of the plan to have a common value of c_1. As mentioned above, for the free jet,

$$\delta_{char} = r_{.5} \tag{28}$$

The characteristic length for the free shear layer was taken as

$$\delta_{char} = z_{.25} - z_{.75} \tag{29}$$

which is the distance normal to the flow in the shear layer from the point where the velocity is one-quarter the external driving velocity to where it is three-quarters this velocity.

In Figures 7 through 14, we show comparisons with experimental data of the velocity correlation profiles computed for both a free jet and a free shear layer, using the model parameters given above. The experimental results are taken from the work of Wygnanski and Fiedler (Refs. 11 and 12), Gibson (Ref. 13), and Donaldson, Snedeker, and Margolis (Ref. 14).

Figures 7 and 8 show the longitudinal fluctuations in a free jet and free shear layer, respectively. The agreement between model calculations and experiment is good in both cases. For the free jet in Figure 7, it would, perhaps, have been desirable to have a little more diffusion (larger Λ_1 and larger b) in the model in an attempt to reduce the overshoot in $\langle w'w' \rangle$ near the centerline of the jet.

Figures 9 and 10 show distributions of normal fluctuations in both the free jet and the free shear layer. Here we note the agreement with experimental data is not so good. There appears to be a little too much diffusion for these cases. Also, note

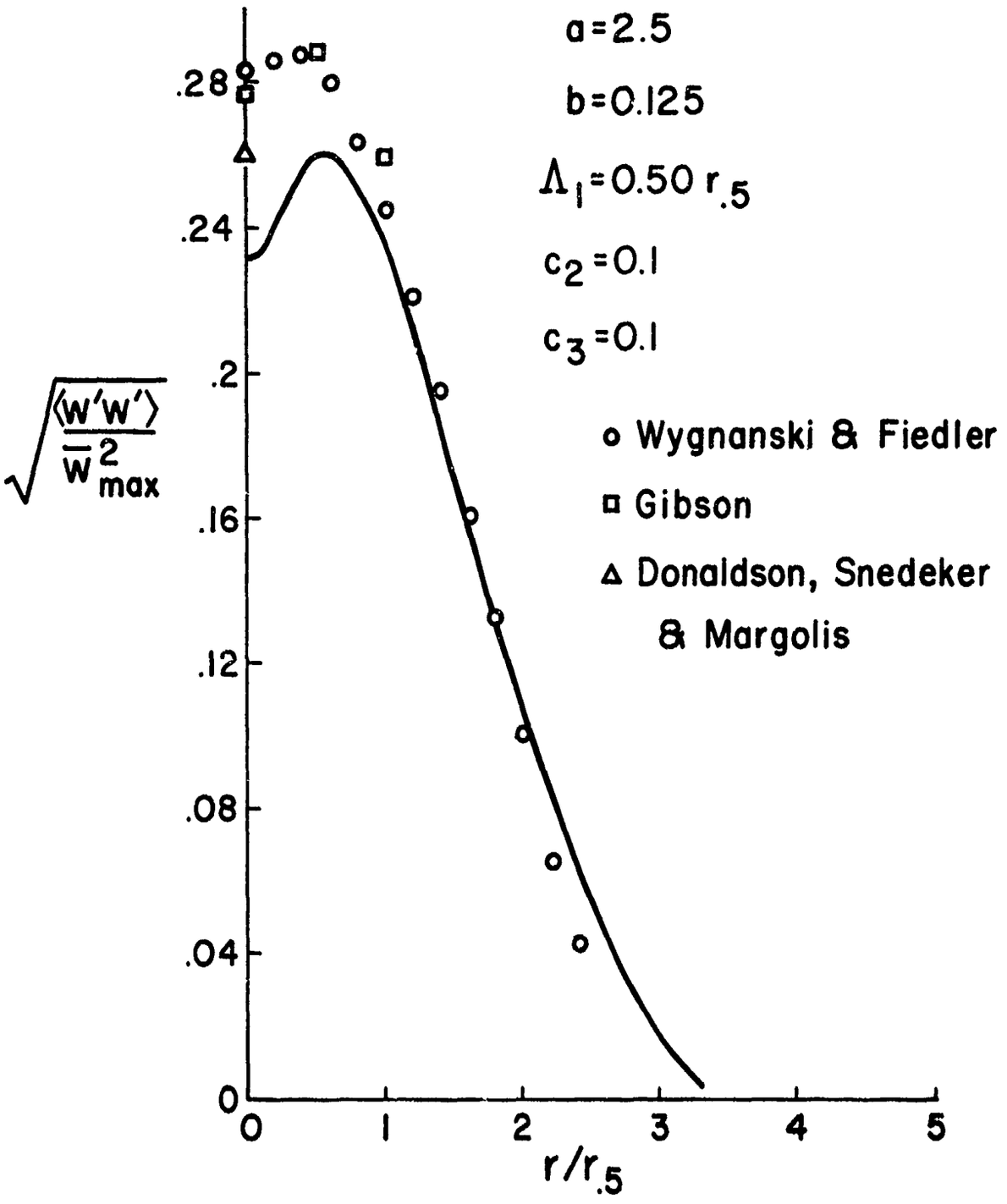

Fig. 7. Comparison of experimental results and model predictions for the longitudinal velocity correlations in a free jet

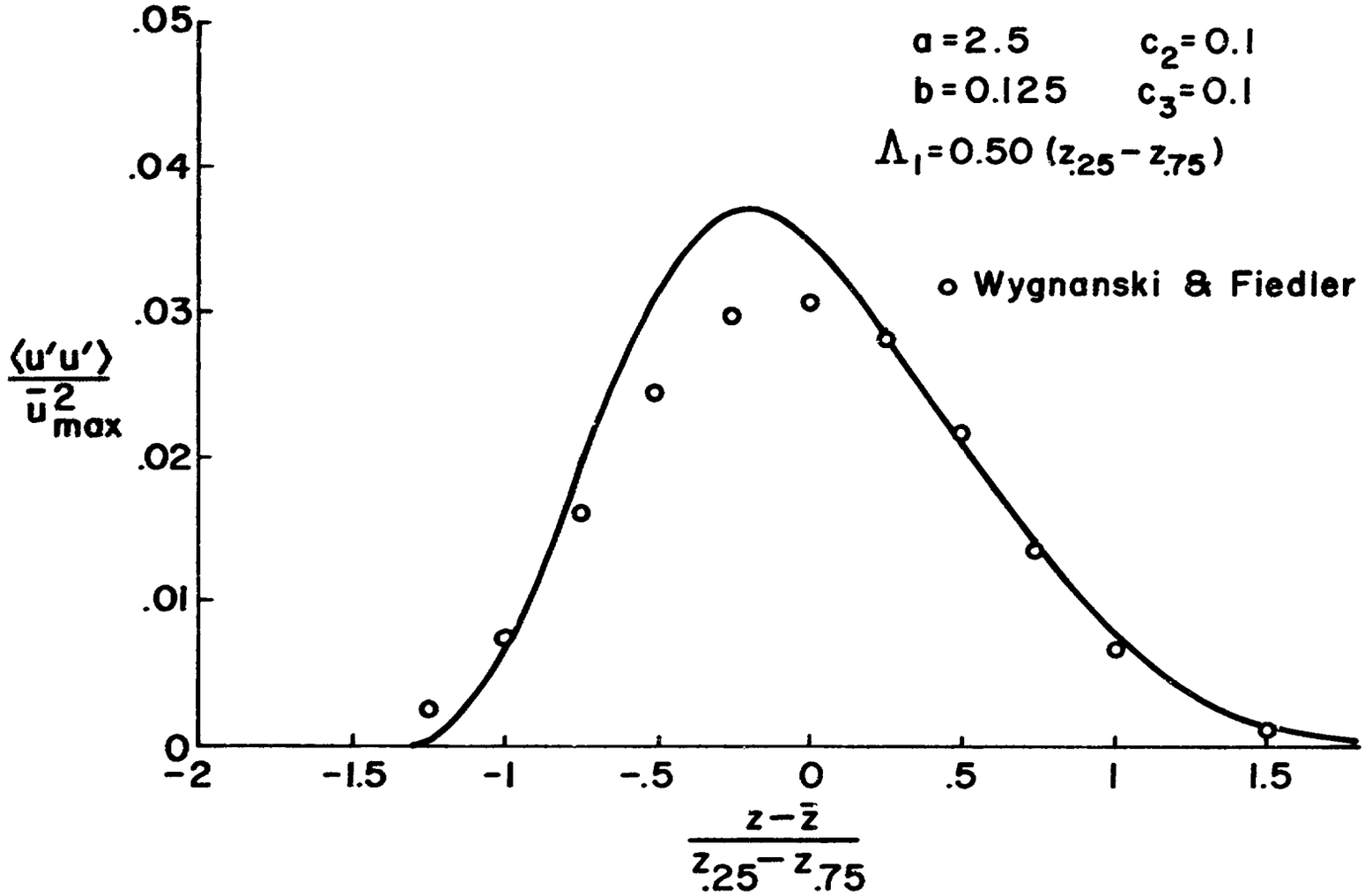

Fig. 8. Comparison of experimental results and model predictions for the longitudinal velocity correlations in a free shear layer

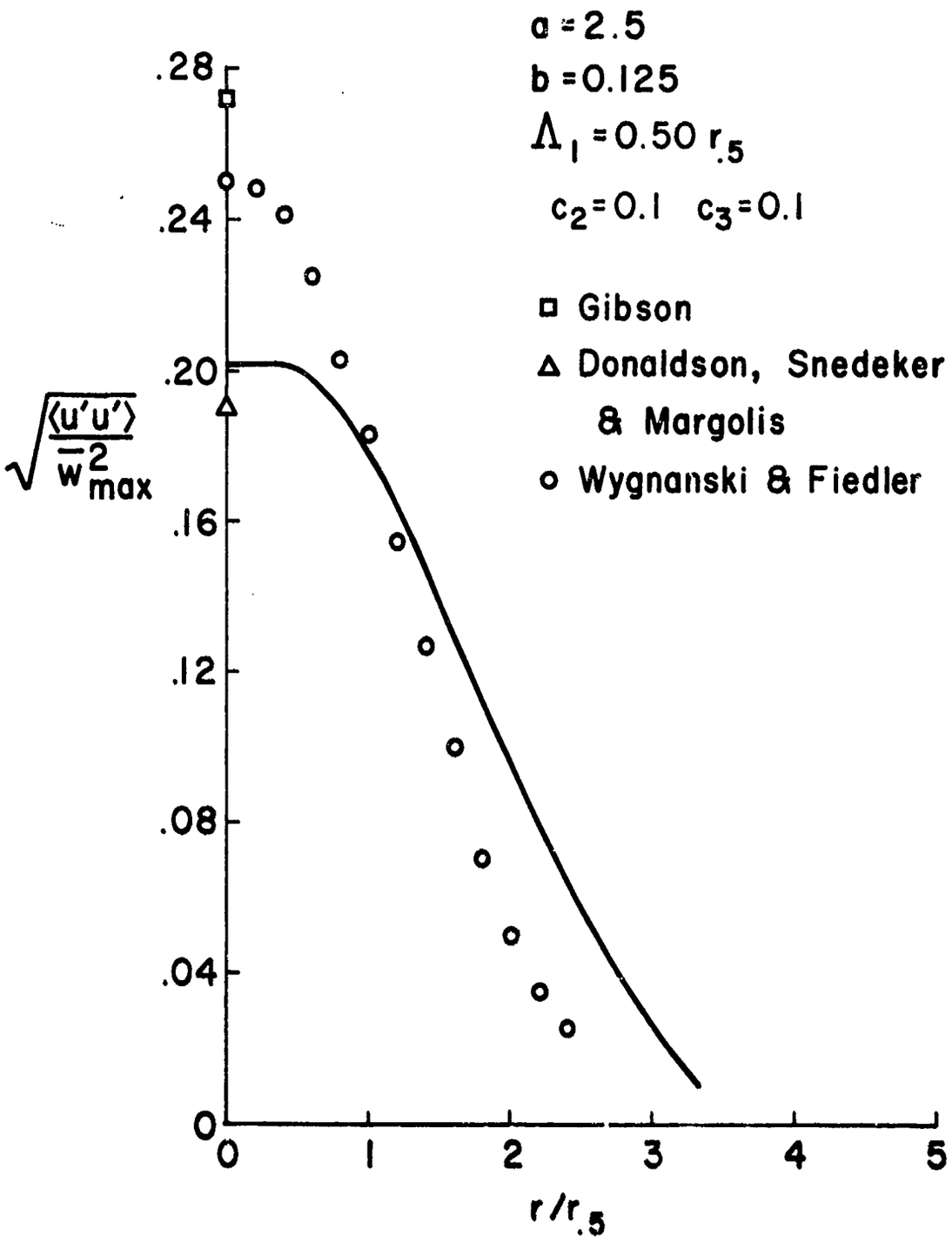

Fig. 9. Comparison of experimental results and model predictions for the radial velocity fluctuations in a free jet

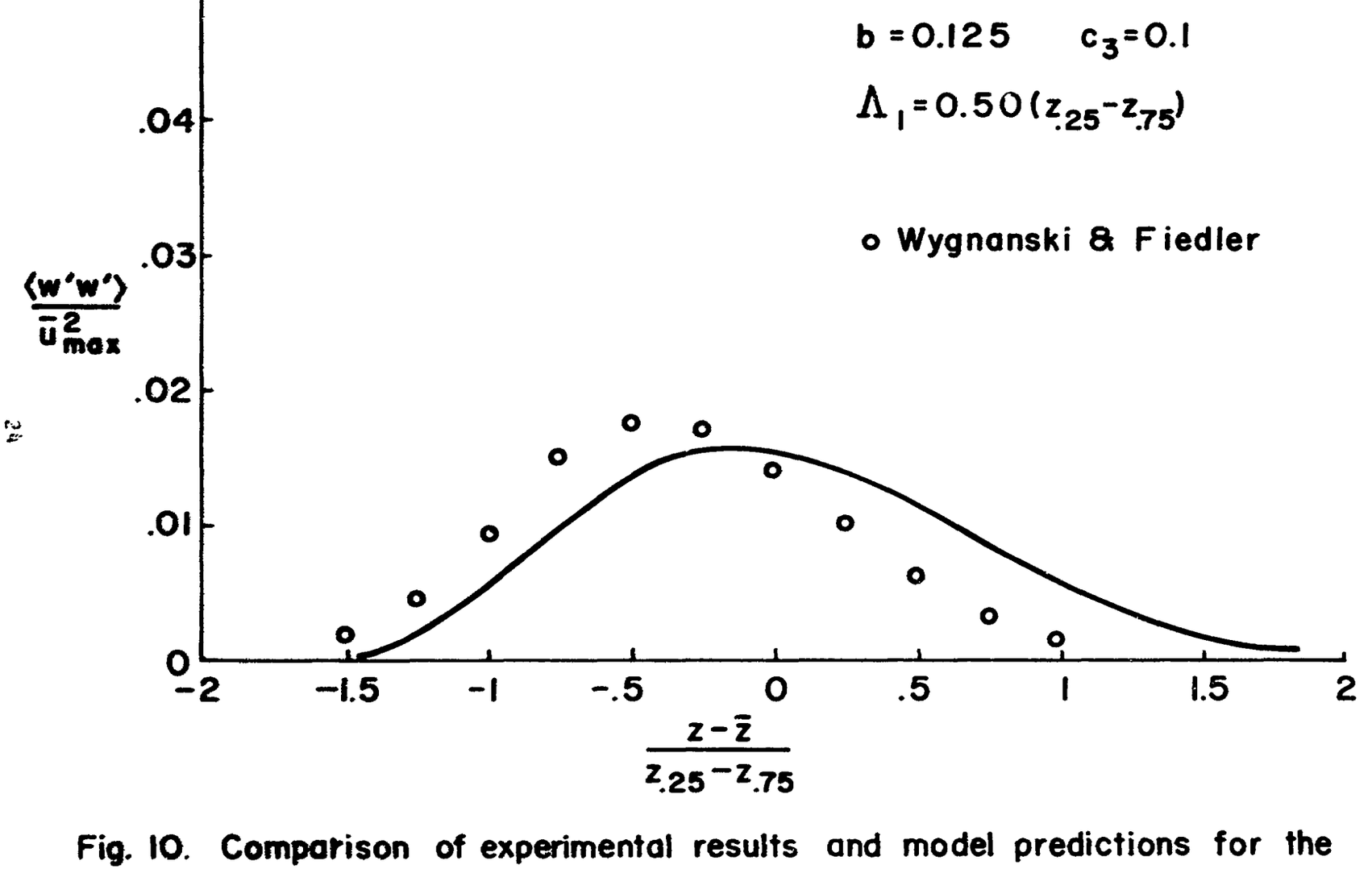

Fig. 10. Comparison of experimental results and model predictions for the normal velocity fluctuations in a free shear layer

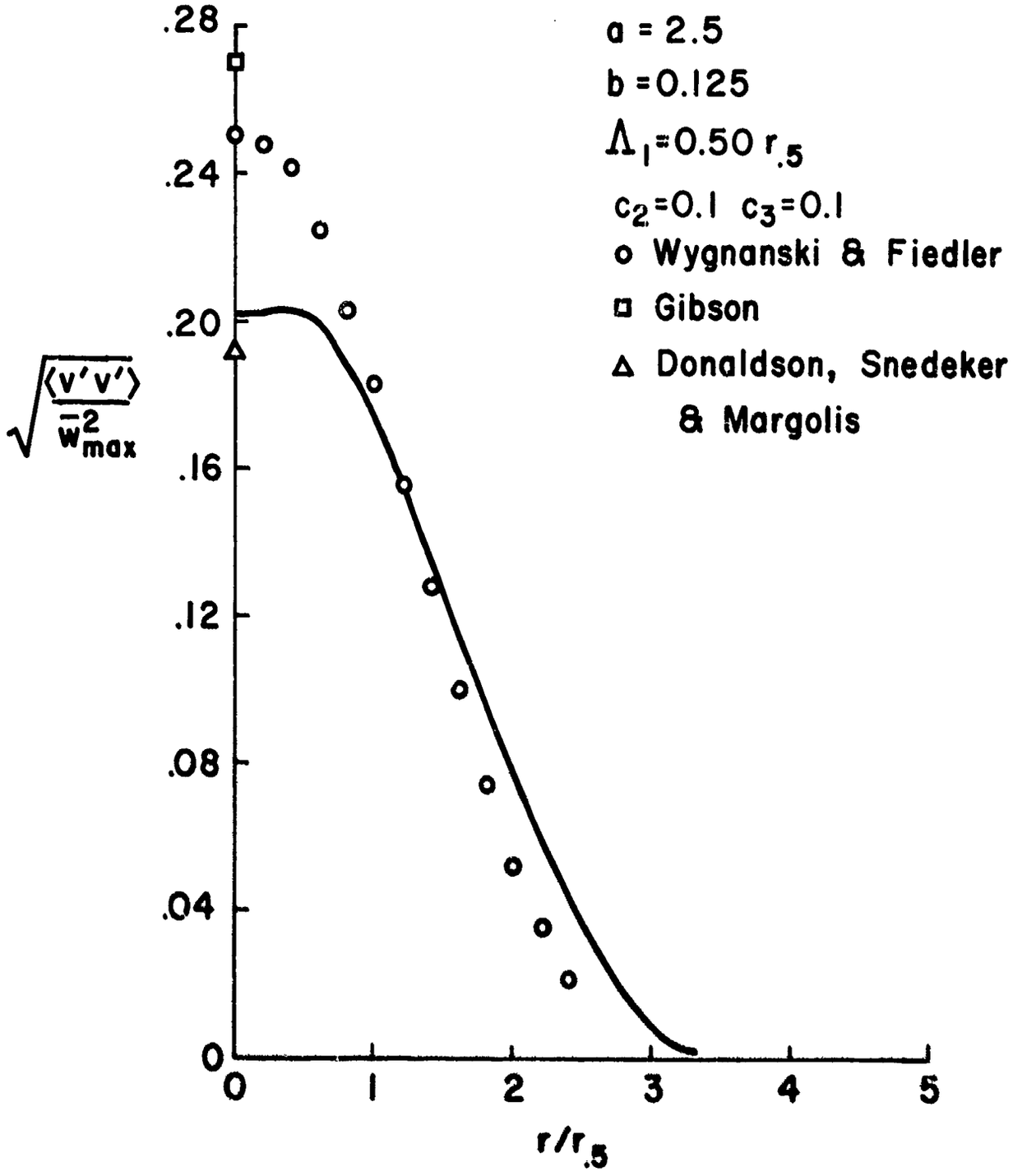

Fig. 11. Comparison of experimental results and model predictions for the sidewise fluctuations in a free jet

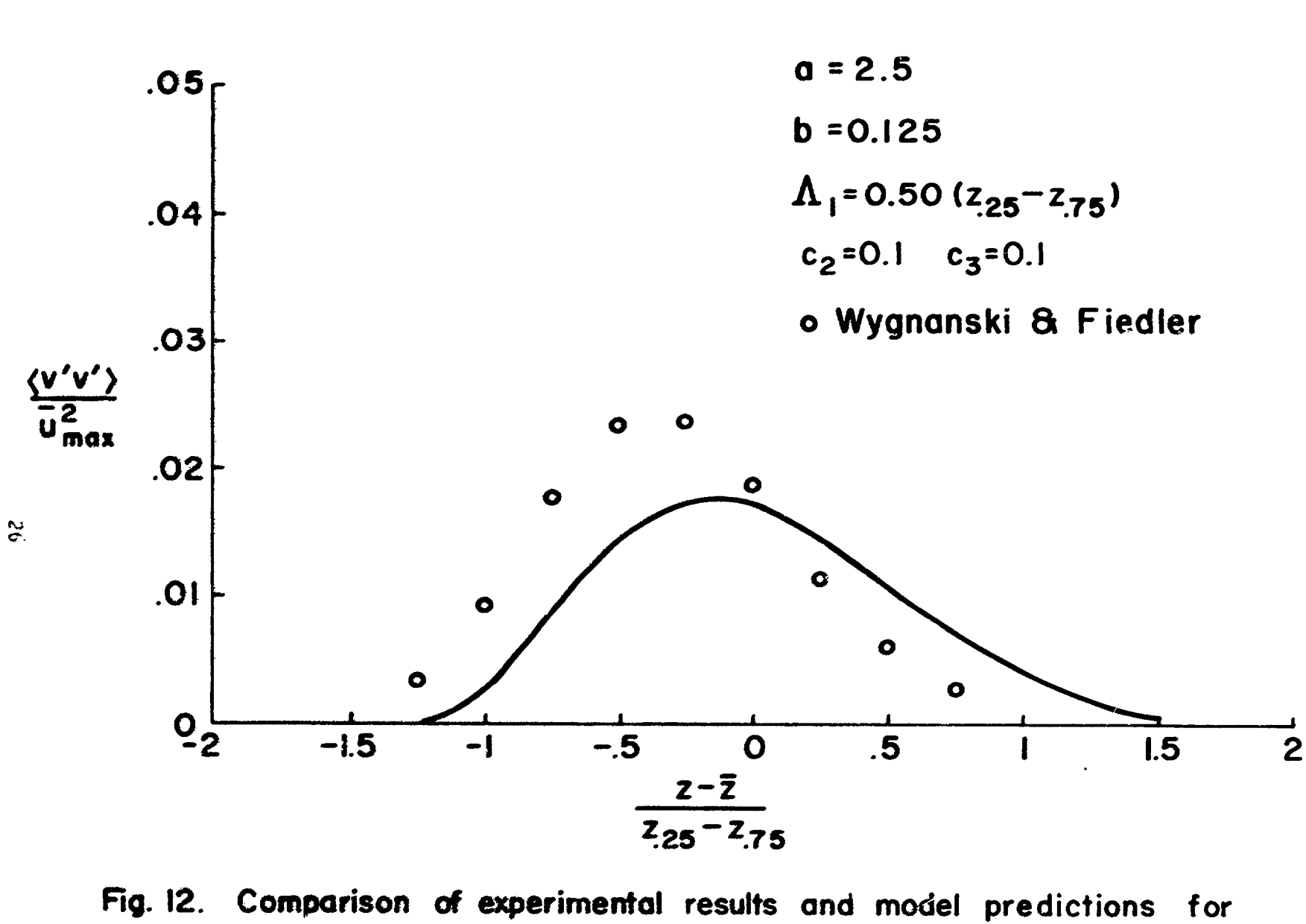

Fig. 12. Comparison of experimental results and model predictions for the sidewise fluctuations in a free shear layer

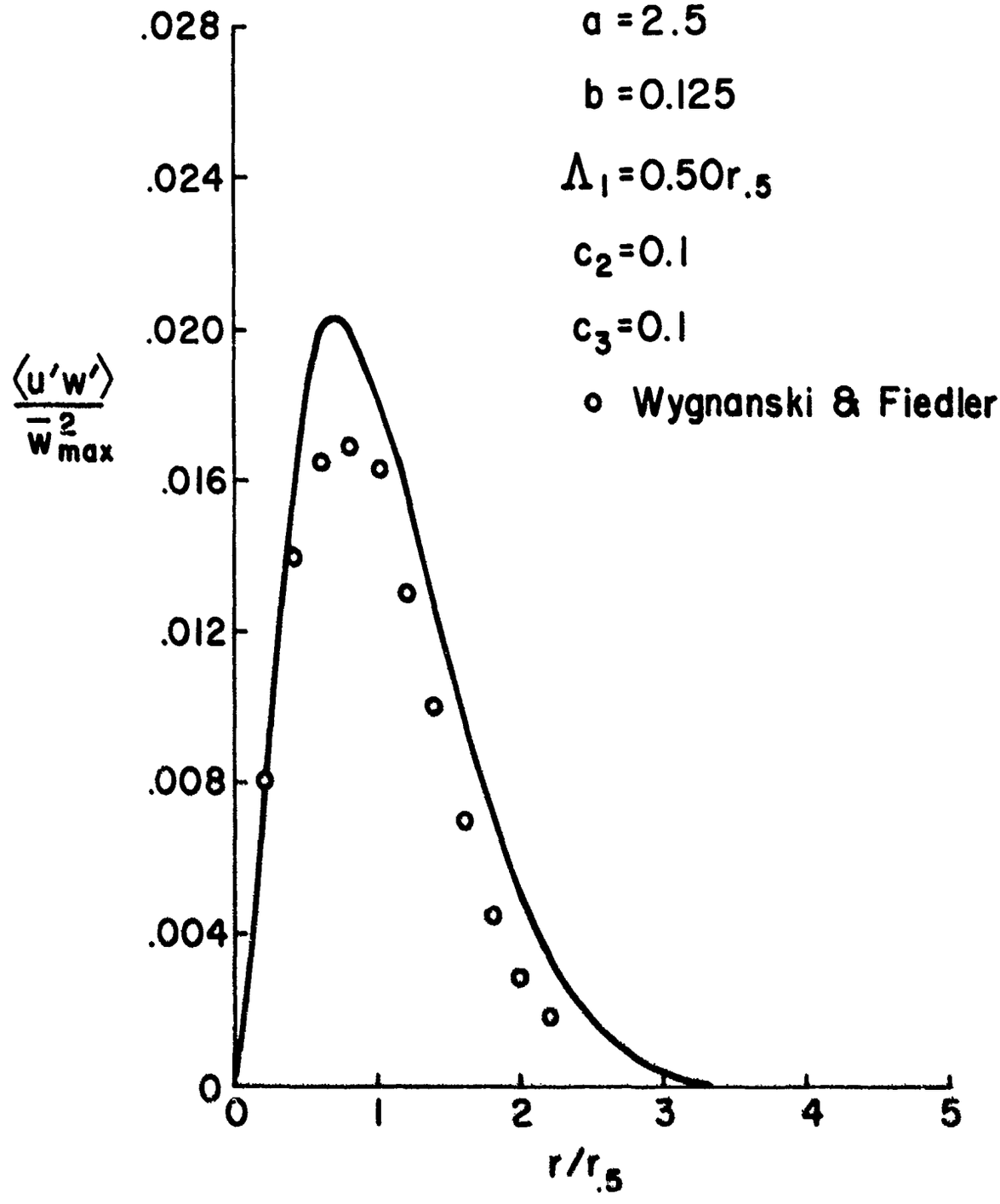

Fig. 13. Comparison of experimental results and model predictions for the shear correlation in a free jet

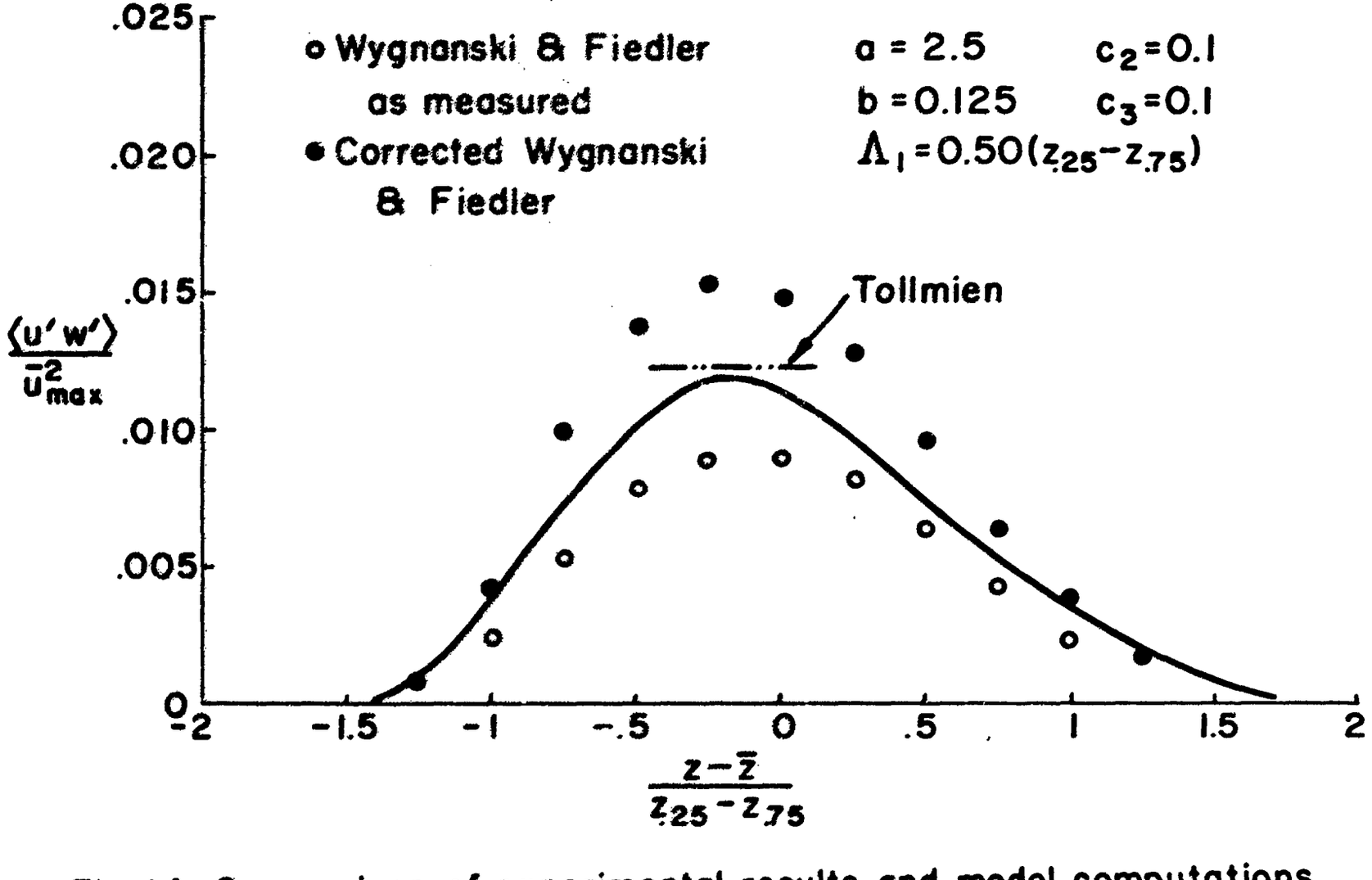

Fig. 14. Comparison of experimental results and model computations for the shear correlations in a free shear layer

the very large discrepancy between measured normal fluctuations on the centerline as reported in three separate experiments. The data of Gibson show the components of turbulent velocity to be essentially isotropic on the jet centerline, while those of Wygnanski and Fiedler and Donaldson, Snedeker and Margolis do not. From the results shown in Figure 9, it would appear that if one were to desire more isotropy, one would wish to choose a smaller value of A_1 and, hence, a smaller value of b. This is opposite to the conclusion drawn from Figure 7.

Figures 11 and 12 show the sidewise components of turbulence for the free jet and free shear layer, respectively. The agreement between experiment and computed results is better for the free jet than for the free shear layer. The reason for this behavior is not known.

In Figures 13 and 14, we show the shear correlations for the free jet and the free shear layer. The agreement in both cases is fair. It should be noted that the experimental values of shear correlation from Ref. 11 have been shown as reported (the open circles) in Figure 14 and also as corrected by us (the solid symbols) so as to agree with the measured rate of spread of the free shear layer. A comparison of the measured shear and that inferred from the mean velocity profile was reported by Wygnanski and Fiedler but apparently their computations contained an error. Also shown in Figure 14 is the level of shear that may be inferred from the mean spread of the free shear layer studied by Tollmien (Ref. 15) and Prandtl (Ref. 16) many years ago. It is seen from the results presented in Figures 13 and 14 that the model gives a fairly good representation of the shear in both the free jet and the free shear layer.

A careful study of Figures 7 through 14 shows that it really is necessary to study further the problem of choice of model parameters. However, before this is done, it appears desirable to have at hand experimental data which one can rely on to be truly representative of the basic flow which is being calculated. It is difficult to choose a more sophisticated model until the question of the degree of isotropy on the centerline of a free jet is settled. In addition, one should, at this point, determine if the model just found for free shear layers can be used for a model of the outer regions of a boundary layer and give reasonable results.

Before turning to the problem of the turbulent boundary layer, it will be instructive to find a relationship between the values of A_1 used in the free shear layer and the free jet calculations and the general magnitude of the integral scales measured for such flows. In the computations that have been made, it has been assumed that A_1 is constant across a free jet or a free shear layer at any given longitudinal position and, in magnitude, proportional to the local scale of the mean flow. It is well known that the integral scales of such flows are, in general, proportional to the local mean scales but the actual value of the integral scale varies across the layer.

In Table 1, we present the values of integral scale within a free jet, as reported by Wygnanski and Fiedler. The integral scale tabulated is the longitudinal integral scale

$$L = \frac{1}{\langle w'w' \rangle (z_1)} \int_0^\infty \langle w'(z_1) w'(z_2) \rangle \, d(z_2 - z_1) \tag{30}$$

for the free jet.

Table 1

Integral Scales in a Free Jet after Wygnanski and Fiedler (Ref. 11)

Radial Position	Dimensionless Scale	Scale Ratio
r/x	$L/r_{.5}$	Λ_1/L
0	0.448	1.12
.05	0.595	0.84
.10	0.726	0.69
.15	0.850	0.59
.20	0.855	0.58

Also presented in Table 1 is the ratio of the computational scale Λ_1 to the local integral scale L. Thus, a typical value for this ratio for the free jet is

$$\Lambda_1/L = 0.69 \tag{31}$$

For the free shear layer, similar results are given in Table 2. These experimental values are also due to Wygnanski and Fiedler. The longitudinal integral scale is, in this case, defined by

$$L = \frac{1}{\langle u'u' \rangle (x_1)} \int_0^\infty \langle u'(x_1) u'(x_2) \rangle \, d(x_2 - x_1) \tag{32}$$

Table 2

Integral Scales in a Free Shear Layer after Wygnanski and Fiedler (Ref. 12)

Location in Jet	Dimensionless Scales		Scale Ratio
	L/x	$L/(z_{.25}-z_{.75})$	Λ_1/L
Inner Region	0.098	0.846	0.59
Center	0.103	0.883	0.57
Outer Region	0.147	1.27	0.39

A typical value of Λ_1/L for a free shear layer appears to be approximately

$$\Lambda_1/L = 0.55 \tag{33}$$

As mentioned previously, there is not much point in going further with studies of the present model until it has been applied to a boundary layer. Note should be made at this point, however, of other methods of calculating turbulent shear flows - methods that are similar to the methods being discussed here. As mentioned before, the idea behind the method is not new. It follows a trend suggested by Prandtl and Wieghardt (Ref. 1) and follows closely the general line of approach taken by Rotta (Ref. 6). Since these two pioneering papers, many more or less similar studies have been undertaken. Typical of many such studies are those of Glushko (Ref. 18), Bradshaw, Ferriss & Atwell (Ref. 19), Harlow & Romero (Ref.20), Gawain & Pritchett (Ref. 21), and Beckwith & Bushnell (Ref. 22). The more sophisticated of these methods do not assume a local scale, as we have, but carry along with the computational scheme an equation for the required scale. Such an equation was derived by Rotta (Ref. 6) from the equation for the two-point correlation tensor $\langle u_i'(A)u_j'(B)\rangle$. There is no question but that, in the future, the method presented here should be enhanced by coupling the present set of model equations to an equation for the integral scale. To date, however, we have avoided making this connection in order to study the character of the model and its dependence on the scale Λ_1 without this dependence becoming inextricably mixed with the additional modeling that must be done in the equation that is used to compute a scale.

Before proceeding further, it must be demonstrated that, if the present model is applied to a boundary layer, useful results will be obtained for the same choice of model parameters that has been made for free turbulent shear flows.

V. APPLICATION OF MODEL TO BOUNDARY LAYERS

If the model of turbulent shear flows is to be applied to a boundary layer, the parameters c_2 , c_3 , a and b are known. But, since the characteristic length in a boundary layer is arbitrary (as it is in the free jet and the free shear layer), we are at liberty to choose c_1 , i.e., the ratio between Λ_1 and the characteristic length (which, in this case, we take equal to $\delta_{.99}$, the thickness of the layer in which the velocity reaches 99% of its free stream value).

As discussed in a previous section of this paper, one other parameter enters the problem, namely, α , the coefficient appearing in Eq.(21). We have, then,

$$\Lambda_1 = \alpha\sqrt{a}\, z \tag{34}$$

for $0 \leq z \leq c_1\delta_{.99}/(\alpha\sqrt{a})$, and

$$\Lambda_1 = c_1\delta_{.99} \tag{35}$$

for $z > c_1\delta_{.99}/(\alpha\sqrt{a})$

With only these two parameters α and c_1 to determine, the search is not difficult. The model that has been found is the following:

$$\begin{aligned} a &= 2.5 \\ b &= 0.125 \\ c_2 &= 0.1 \\ c_3 &= 0.1 \\ c_1 &= \Lambda_1/\delta_{.99} = 0.15 \\ \alpha &= 0.7/\sqrt{a} = 0.443 \end{aligned} \tag{36}$$

The ability of this model of a turbulent shear layer to predict the known mean properties of turbulent boundary layers is shown in Figures 15 through 17. In Figure 15, we show the skin friction developed by our model as it proceeds from a disturbed laminar layer to a fully turbulent layer. Also shown are the laminar skin friction law and the turbulent law proposed by Coles (Ref. 23) which is a good fit to experimental data. It is no great surprise that the general levels of skin friction we computed agree well with experimental findings inasmuch as the values of α and c_1 were chosen to get these levels correct. Of more importance is the nearly exact following of the trend of skin friction with Reynolds number by the model computations.

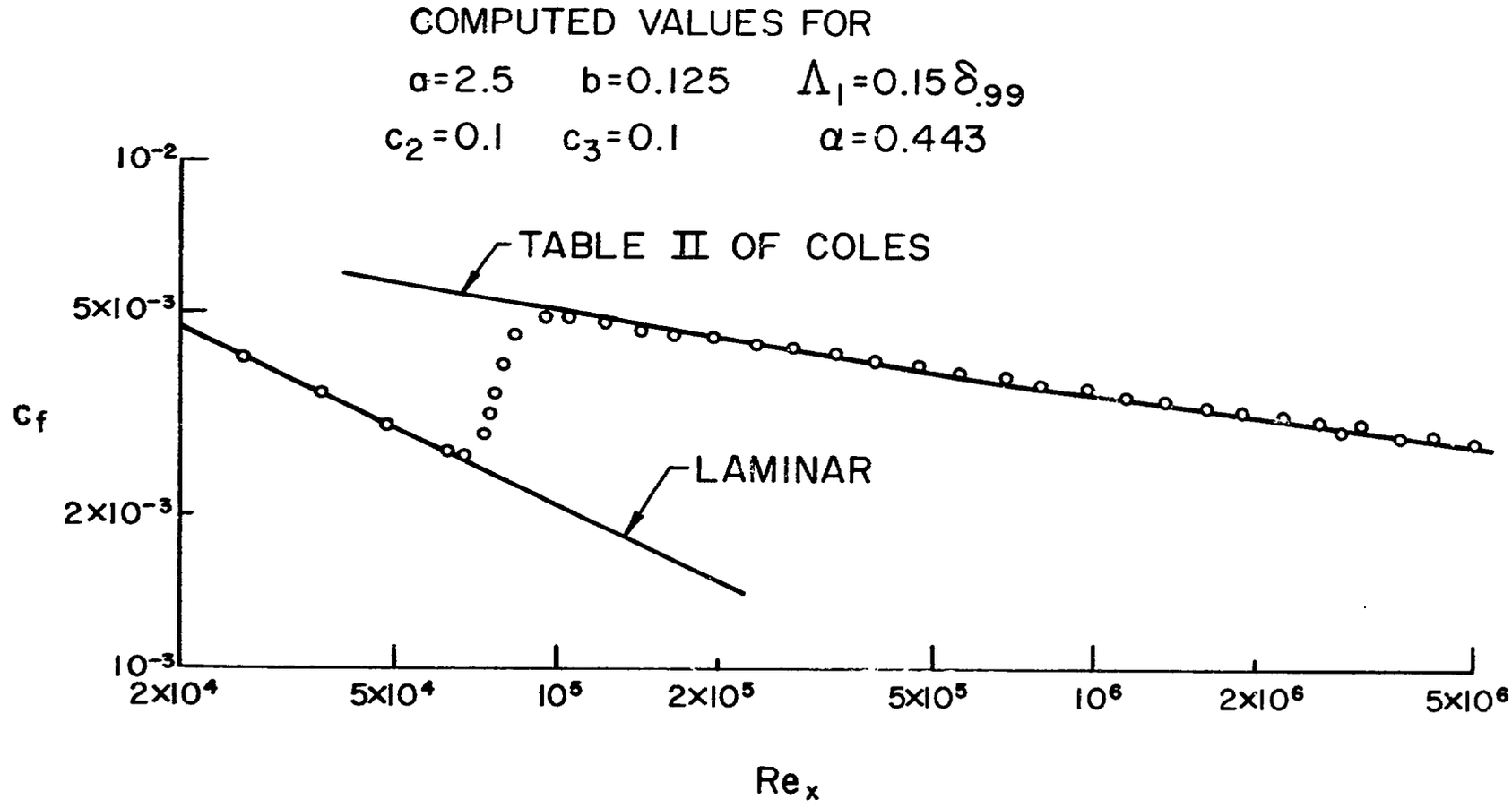

Fig. 15. Computed variation of coefficient of friction with Reynolds number

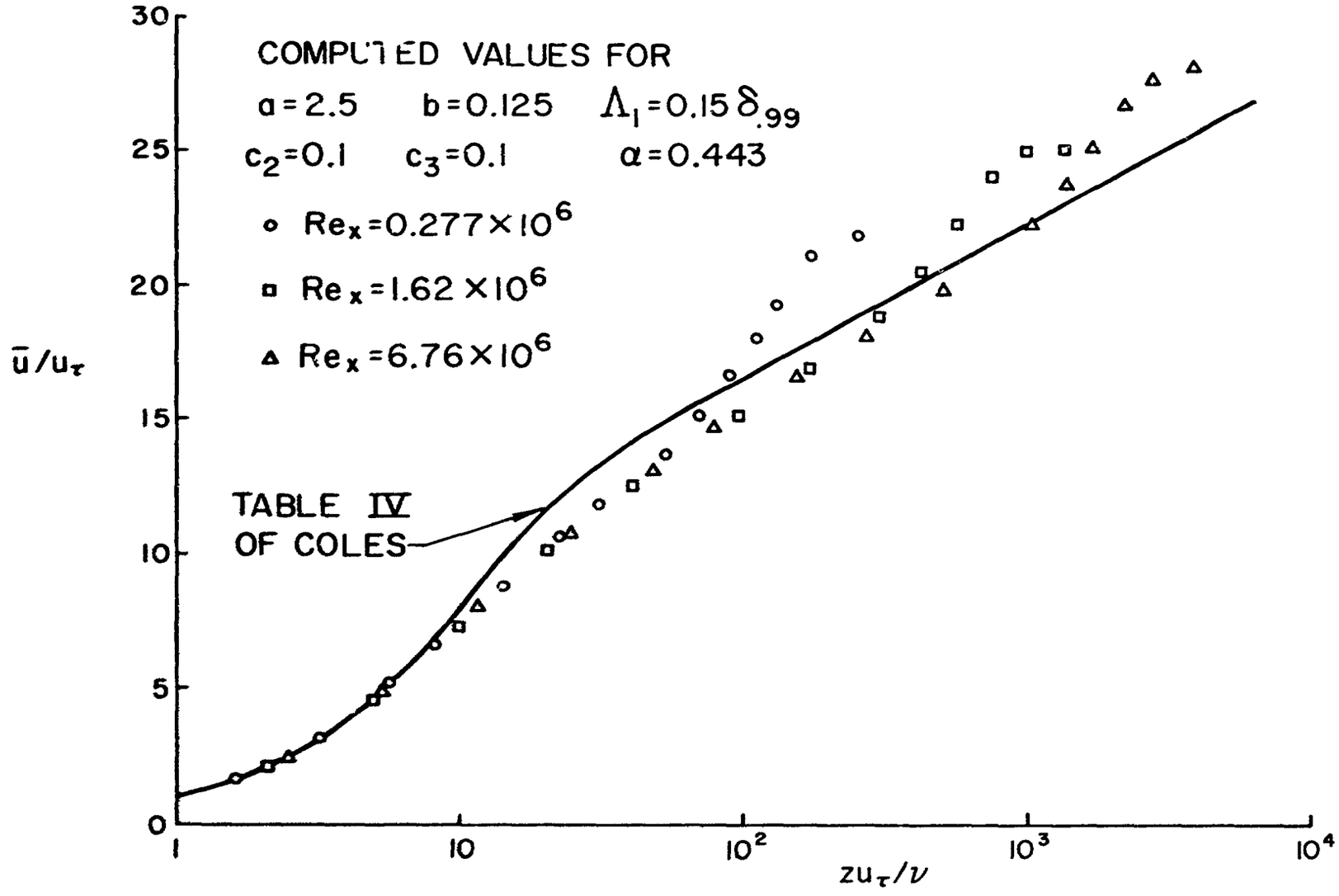

Fig. 16. Computed velocity profiles for three Reynolds numbers. Computation started at $Re_x = 20{,}000$. The reference velocity u_τ is defined by $\tau_{wall} = \rho u_\tau^2$.

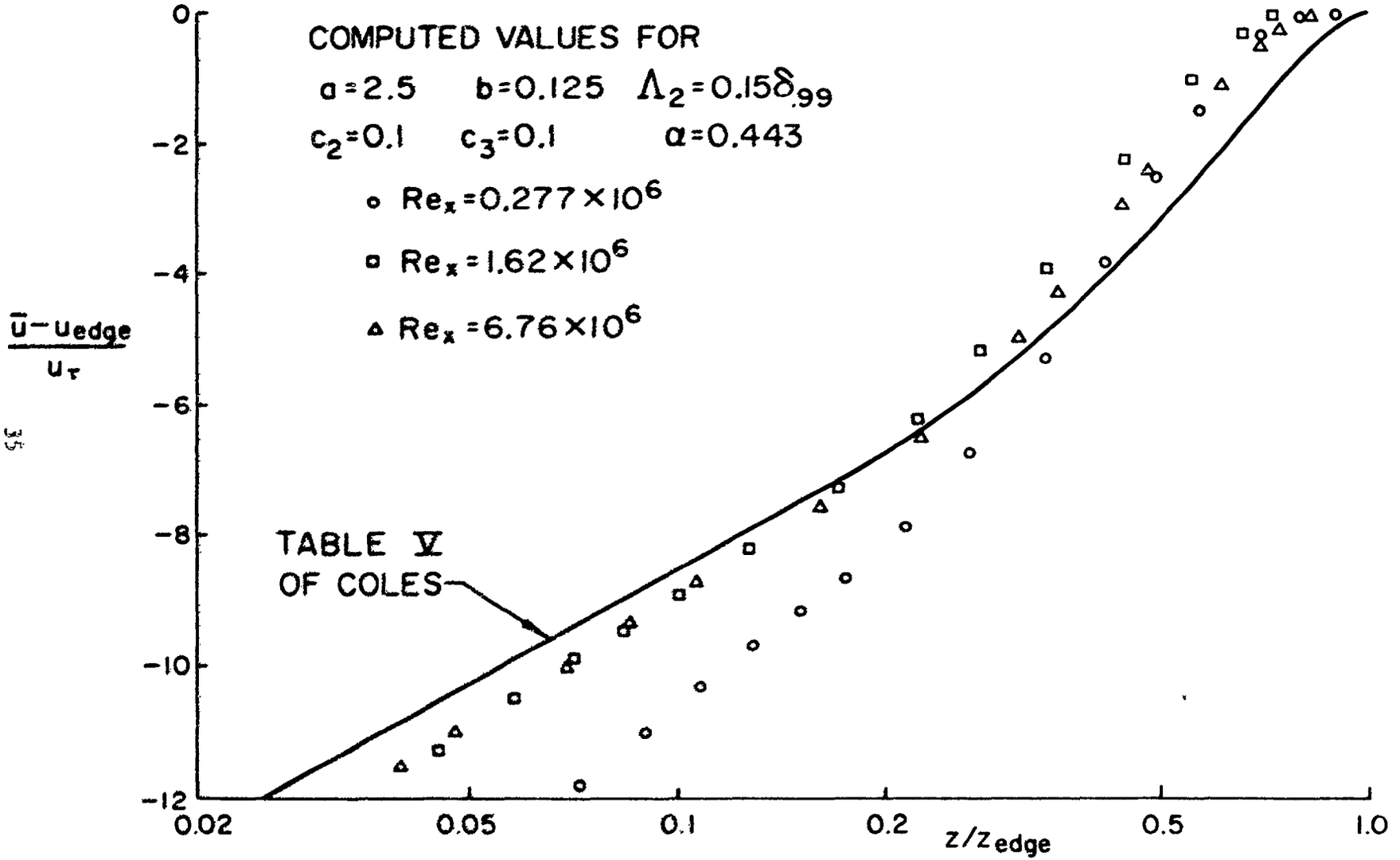

Fig. 17. Computed velocity defects for three Reynolds numbers. Computation started at Re_x=20,000. The reference velocity u_τ is defined by $\tau_{wall}=\rho u_\tau^2$.

Figure 16 shows a comparison of the computed mean velocity profiles developed by the model in the vicinity of the wall and the well-known law of the wall as proposed by Coles (Ref. 23). It may be seen that the law of the wall is not quite achieved by the present selection of model parameters. The results, however, are sufficiently accurate to be encouraging.

In Figure 17 we compare the experimentally determined velocity defect law proposed by Coles (Ref. 23) with the results of our model computations. It is seen that, once the turbulent boundary layer is well established, the computational model gives a fairly good representation of the outer regions of the turbulent boundary layer.

With these results in hand, we must now consider the relationship of the computational scales used to the longitudinal integral scales that are found in the outer regions of turbulent boundary layers. For this purpose, we may use the measurements of Grant (Ref. 24). When the experimental correlations reported by Grant for $y/\delta_o = 0.66$ * in a turbulent boundary layer are integrated to give the longitudinal integral scale, one obtains $L/\delta_o \approx 0.3$. Since for our calculations, $\delta_o/\delta_{.99} = 0.83$, we find that $L/\delta_{.99} \approx 0.25$. Since the computational scale used was $\Lambda_1/\delta_{.99} = 0.15$, we find that

$$\Lambda_1/L \approx 0.6 \tag{37}$$

This is a most welcome result since it shows that, for all the turbulent flows we have investigated, the ratio of the proper computational scale to the longitudinal integral scale is approximately the same.

*Grant defined δ_o as that height in the boundary layer where the velocity defect law was equal to the friction velocity.

VI. CALCULATION OF ATMOSPHERIC TURBULENCE

We may now turn to our original problem, namely, that of computing atmospheric turbulence. In Ref. 2, the equations for the generation of atmospheric turbulence were given and computations were made for some simple shear layers, using the originally determined model parameters [Eqs.(24)]. The model equations for the calculation of atmospheric turbulence using the latest modeling are given in Appendix D.

In what follows, we will turn our attention to a calculation of a case for which atmospheric turbulence has been observed and measured by an instrumented aircraft and for which data were taken on the mean state of the atmosphere nearby, at a time reasonably close to the time of the observation.

In searching the records available from the LO-LOCAT Phase III atmospheric turbulence study, it was decided that an appropriate LO-LOCAT run on which to make our study was leg 5 of Test 43 (Category 422224). In Figure 18 we reproduce from Ref. 25 the normalized atmospheric spectrum Φ_w determined from this particular leg of Test 43. The spectrum is complete enough so that both the turbulent intensity and a longitudinal integral scale can be estimated. We shall treat this spectrum as a partial spectrum, i.e., as if only the $\Psi(\Omega) \sim \Omega^{-5/3}$ power portion of this spectrum was available. Using only this information and the information available from the state of the atmosphere, we will attempt to estimate the values of $\sigma_w = \sqrt{\langle w'w' \rangle}$ and L by calculation of the turbulence that can be produced by the atmosphere for various values of the scale L.

The log for this flight leg on 20 September 1968 shows (Ref. 26):

Time	Mid-morning
Airspeed (true)	614.7 feet/sec
Altitude	775.7 feet
Ambient temperature	69.0°F
Ground temperature	92.7°F
Wind speed	33.5 feet/sec
Wind direction (true) at 750 feet	169°

The state of the winds at the flight altitude is shown in Figure 19.

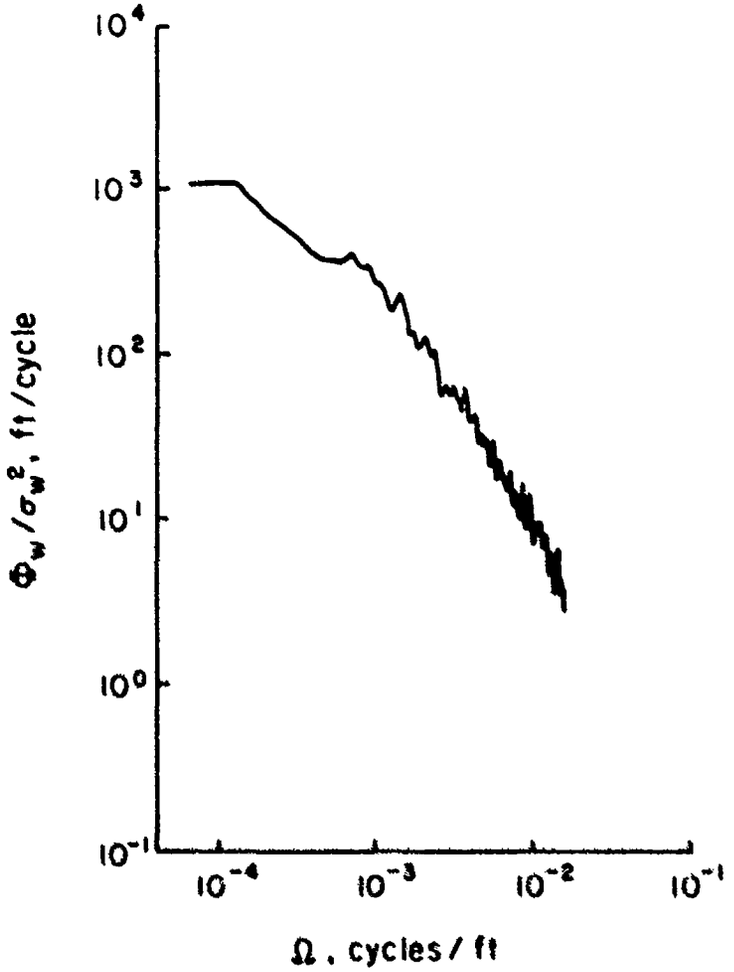

Fig. 18. Normalized power spectrum for Test 43, Leg 5 (Ref. 25)

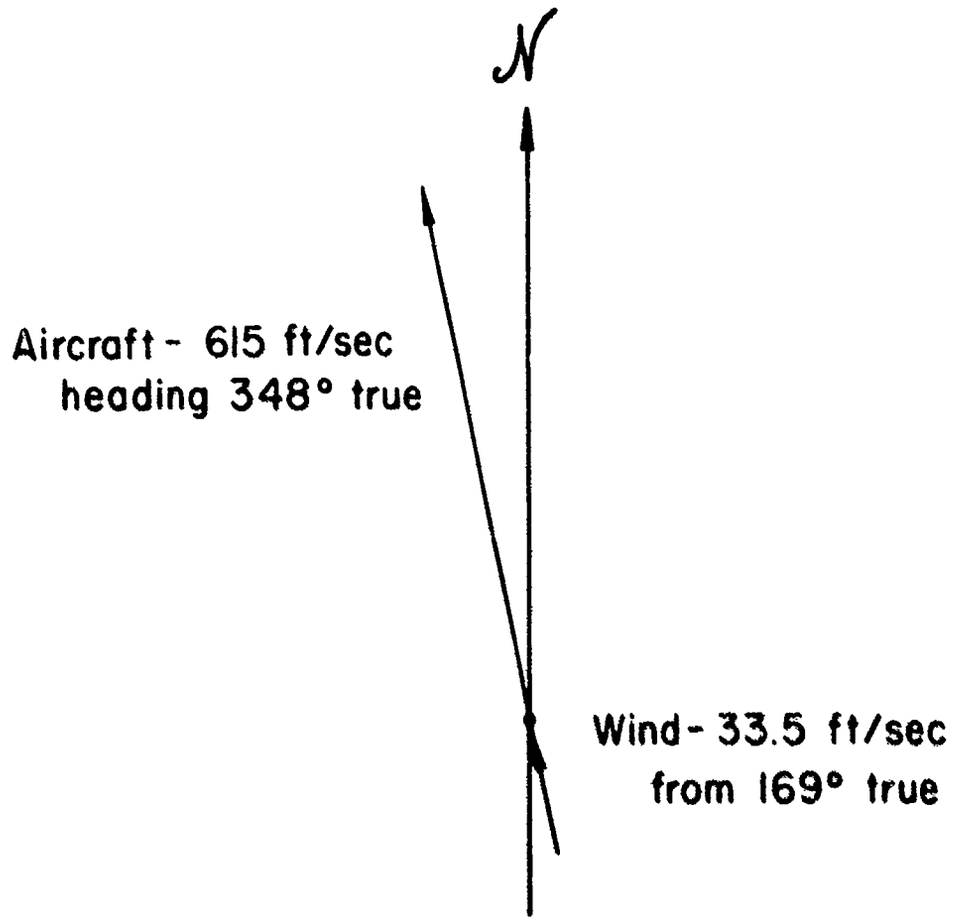

Fig. 19. Wind and aircraft velocities at flight altitude, Test 43, Leg 5 (Ref. 26)

Meteorological data gathered at 0900 hours local standard time on the same day at a point about 15 miles from the flight leg are available (Ref. 27). These data have been plotted in Figure 20; shown are mean velocity and mean temperature measurements deduced from the data, with lines faired through the points to define an atmospheric mean velocity and mean temperature profile. Also shown are the ground temperature and ambient (at 750 feet) temperature and wind velocity as recorded in the flight test log. The considerable discrepancies are to be expected, given the distance and time intervening.

In Figure 21 the temperature profile has been replotted to show the departure of the local temperature from an adiabatic temperature profile. It will be seen that the temperature profile is such that it is unstable from the ground to a height of some 900 feet; thereafter the temperature profile is stable in the region of interest.

Using these profiles, the equations for the development of atmospheric turbulence presented in Appendix D can be solved for the turbulence that will be generated. The only free parameter in the model is the computational scale Λ_1. From the discussion presented in previous sections, we will assume, for these calculations, that this scale behaves as follows.

Near the ground, the scale Λ_1 is given by the formula

$$\Lambda = \alpha \sqrt{a}\, z = 0.7z$$

It will behave in this manner until it reaches some arbitrarily assumed upper limit Λ_1^*. Above this altitude, Λ_1 is assumed to be constant with altitude and equal to Λ_1^*.

Although we know that the integral scale and, hence, the computational scale Λ_1 generally increase with altitude, it is believed that, since we are interested here in a computation of turbulence in only the lower levels of the atmosphere, the assumption of Λ constant above the level of large ground interaction will be adequate.

Computations were carried out for a range of values of Λ_1^* equal to 60, 100, 200, 300, and 400 feet. In Figures 22 and 23, the profiles of $\langle u'u' \rangle$, $\langle v'v' \rangle$, $\langle w'w \rangle$, and the shear correlation $\langle u'w' \rangle$ are plotted as a function of altitude for values of Λ_1^* of 100 and 200 feet, respectively. For completeness, we also show in Figures 24 and 25 plots of the profiles of the temperature flux correlations $\langle u'T' \rangle$ and $\langle w'T \rangle$ as well as values of the temperature variance $\langle T'^2 \rangle$.

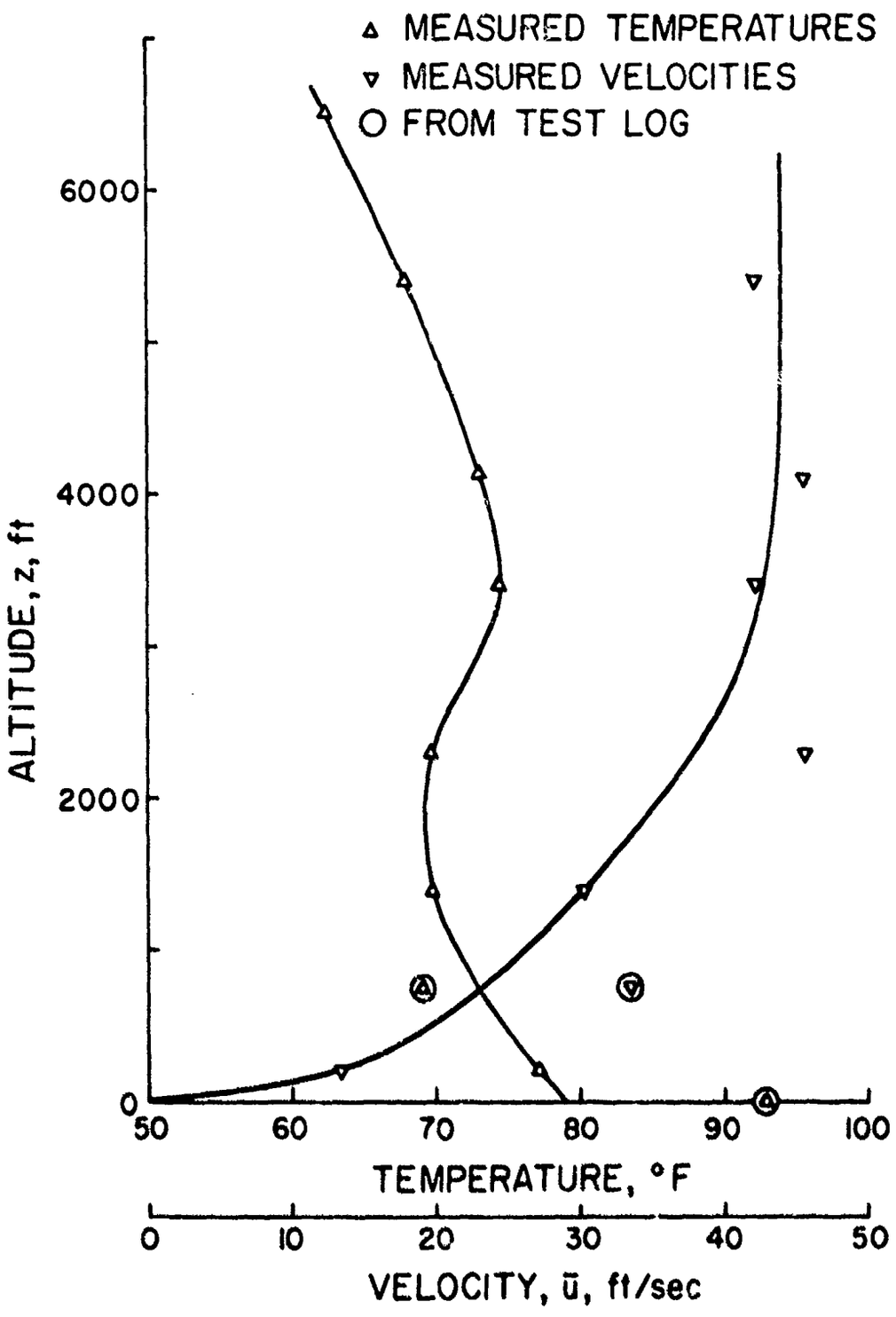

Fig. 20. Reported wind and temperature values from Ref. 27, along with test leg values (Ref. 26)

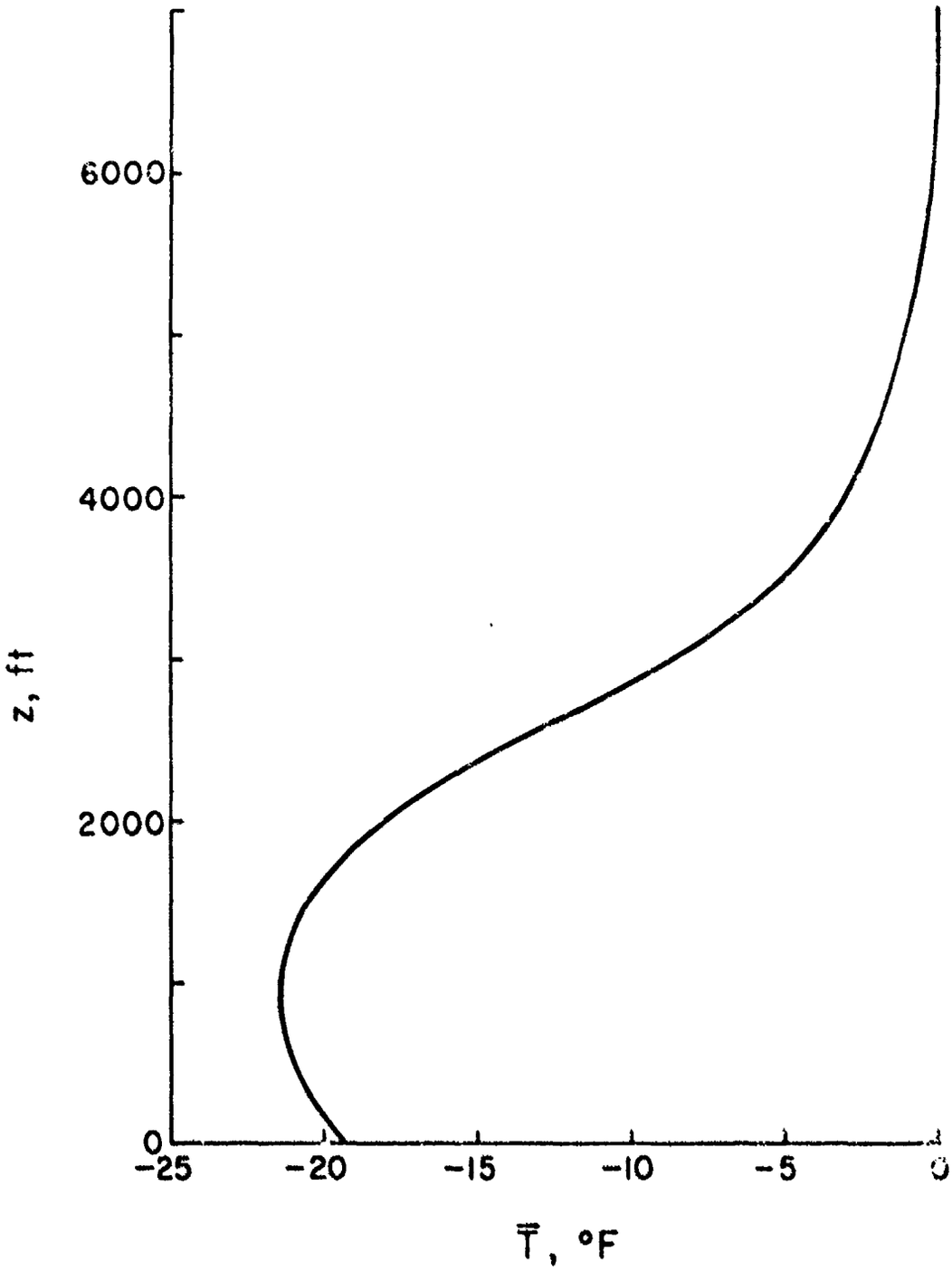

Fig. 21. Difference between actual temperature profile and an adiabatic temperature profile

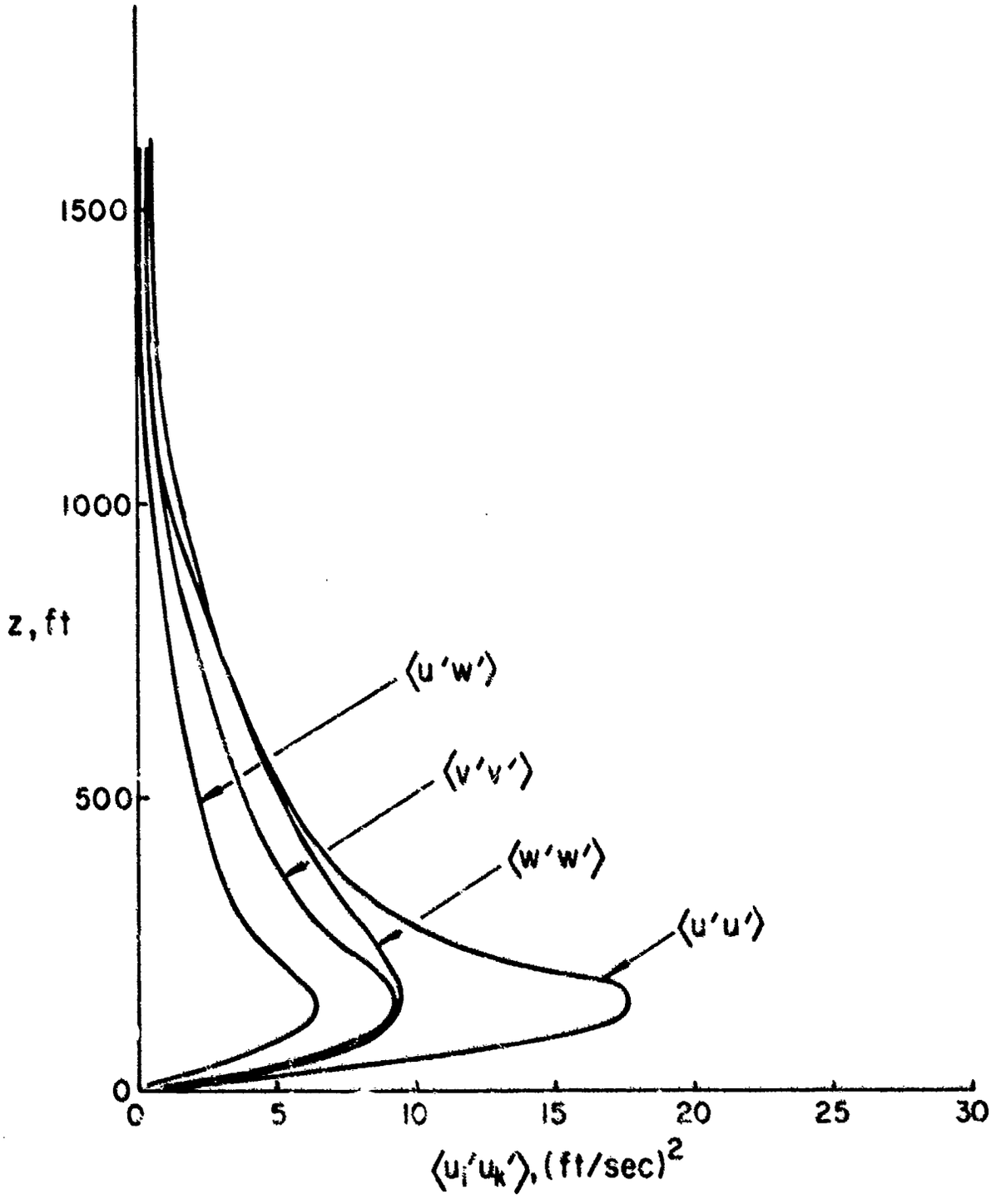

Fig. 22. Computed profiles of stress tensor components for $\Lambda_1^* = 100$

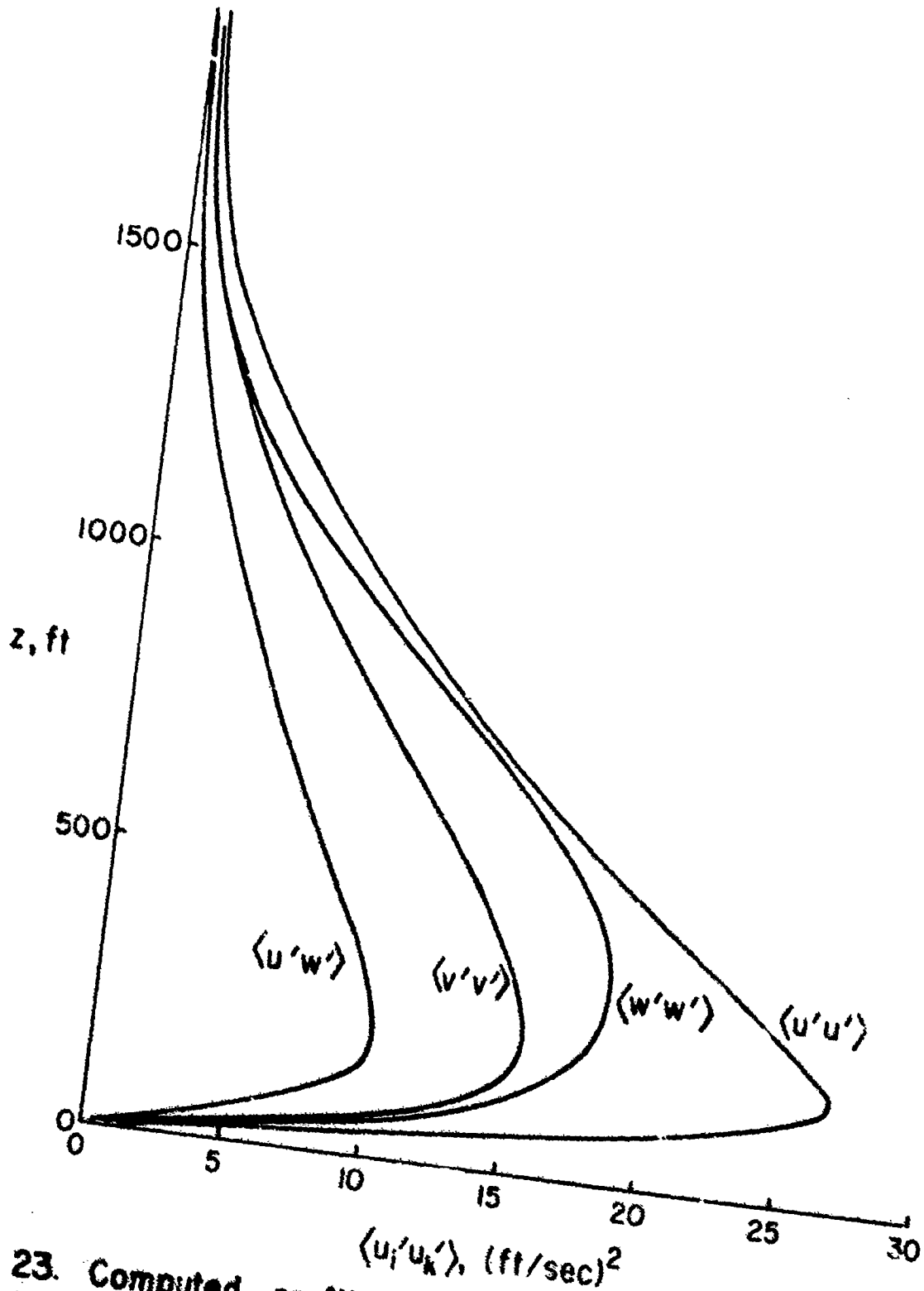

Fig. 23. Computed profiles of stress tensor components for $\Lambda_1^* = 200$ ft

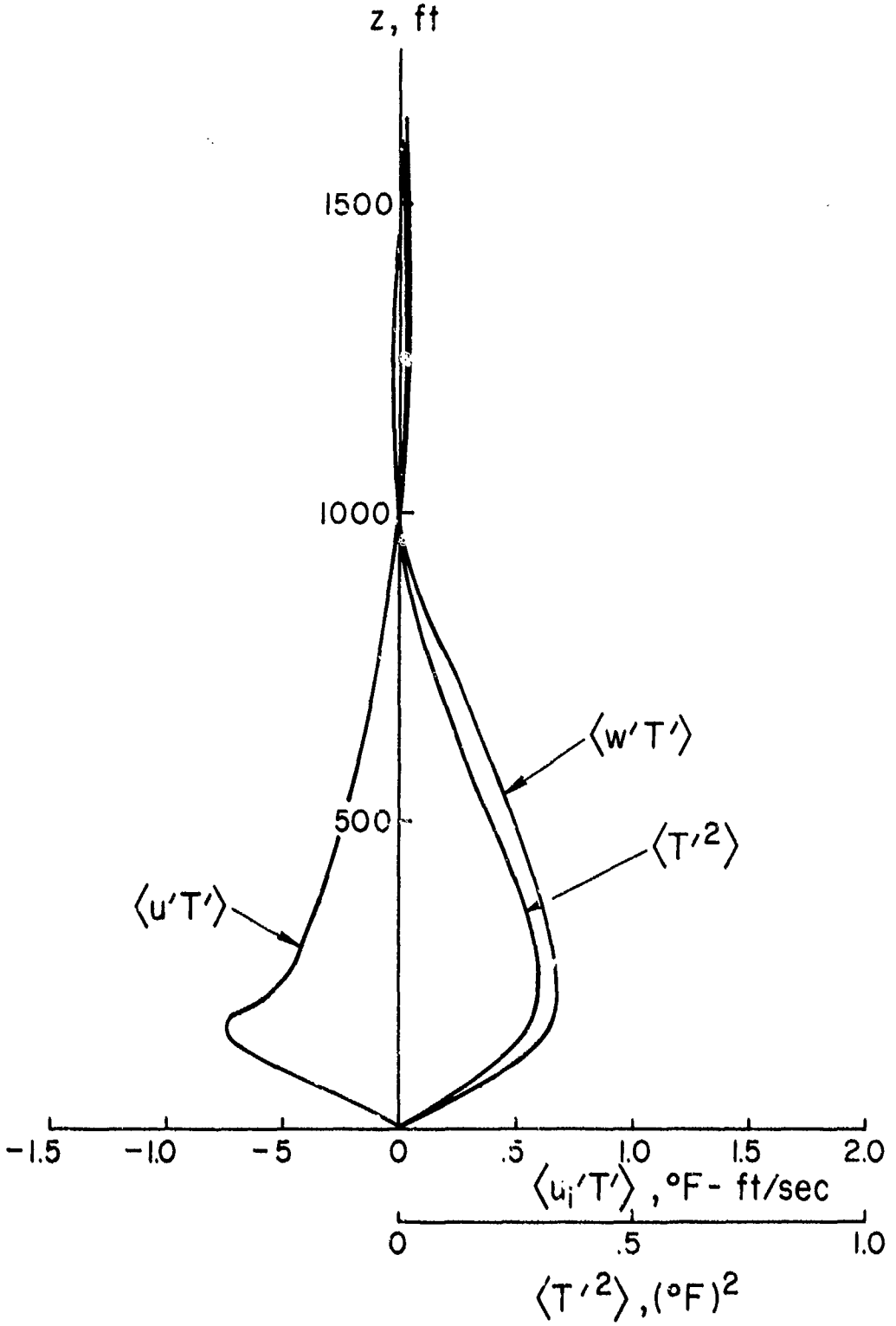

Fig.24. Computed profiles of temperature correlations for $\Lambda_1^* = 100$ ft

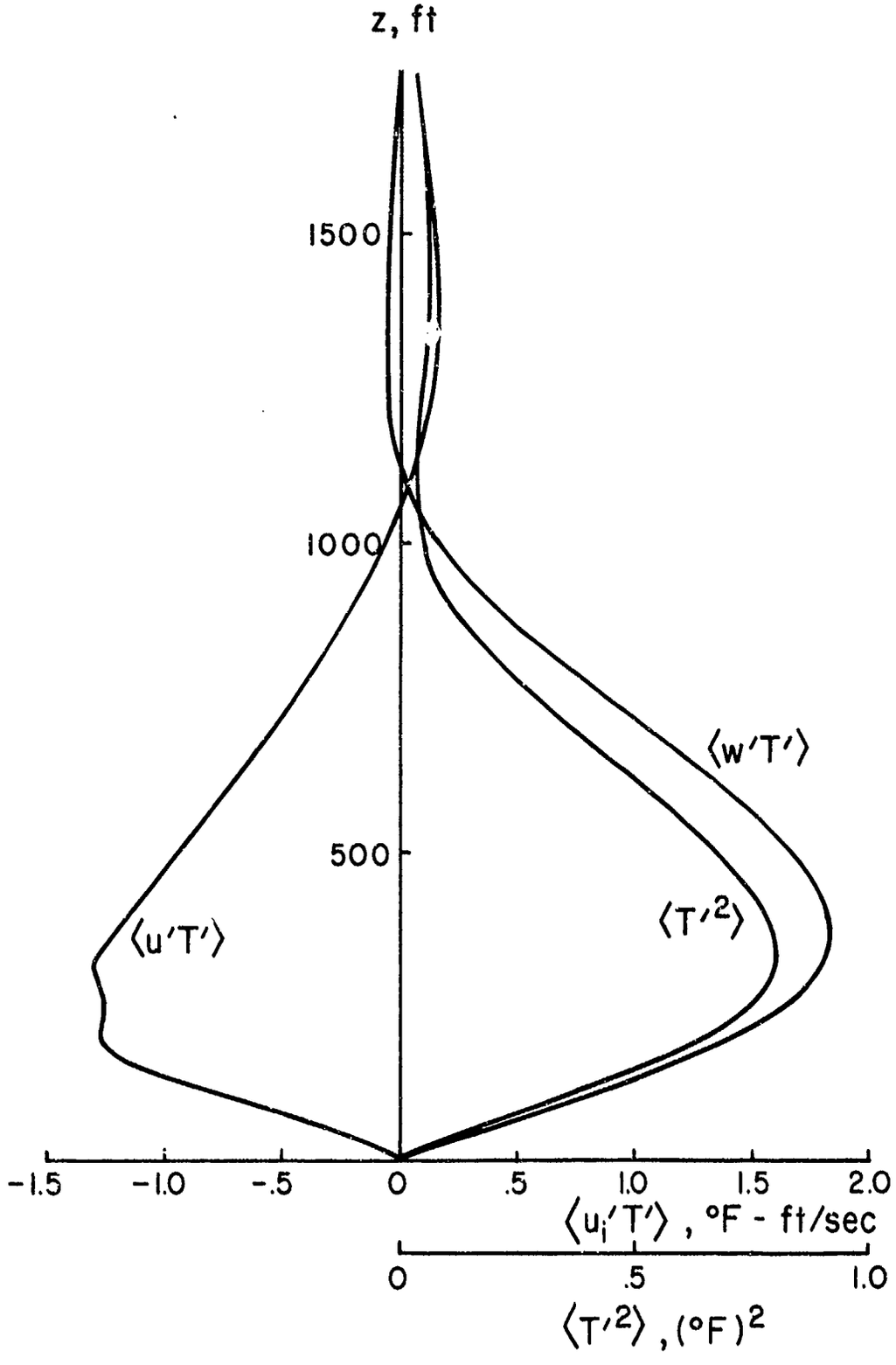

Fig. 25. Computed profiles of temperature correlations for $\Lambda_1^* = 200$ ft

If, from results such as those plotted in Figures 22 and 23, one determines the values of $\sigma_u = \langle u'u' \rangle^{1/2}$, $\sigma_v = \langle v'v' \rangle^{1/2}$, and $\sigma_w = \langle w'w' \rangle^{1/2}$ at the flight altitude (750 feet), a plot of these values as functions of the outer integral scale Λ_1^* can be constructed. Such a plot is shown in Figure 26. The very pronounced effect of the scale Λ_1^* on the magnitude of the turbulence that can be developed is exhibited.

We must now compare these results with the spectral results already discussed. In comparing the three values of Λ_1/L determined previously, namely, 0.69 for the free jet, 0.55 for the free shear layer, and 0.60 for the boundary layer, we select the relationship

$$\Lambda_1 = \Lambda_1^* = 0.60L$$

as representative.

In Figure 27 we show σ_w again as a function of Λ_1^* as in Figure 26 and as a function of L. Also shown is a curve of the relationship between σ_w and L [$\sigma_w \sim L^{1/3}$, according to Eq. (5)] obtained from the spectrum shown in Figure 18, treated as a partial spectrum. We note that the two curves intersect at $\sigma_w = 3.0$ ft/sec and $L = 290$ feet. This may be compared with the results obtained from the complete spectrum (Ref. 25), namely, $\sigma_w = 2.84$ ft/sec and $L = 273$ feet.

The remarkable agreement between these results must be considered fortuitous in view of the many uncertainties involved in constructing wind and temperature profiles for input to our program from the few measurements points available and, more particularly, in assuming these values apply some 15 miles away at a different time. The discrepancies shown in Figure 20 between the two sets of measurements give an indication of the validity of our results.

Although the agreement we have just found is better than expected and, certainly, additional calculations of the type we have just presented must be carried out, we do believe we have demonstrated a method of computing atmospheric turbulence that has sufficient merit to warrant further investigation and development. The other conclusion that one can draw from the calculation that we have presented is that, in the future, it would be most desirable to expend every effort to obtain measurements of the mean state of the atmosphere as close in time and space to any actual flight measurements of turbulence as is possible.

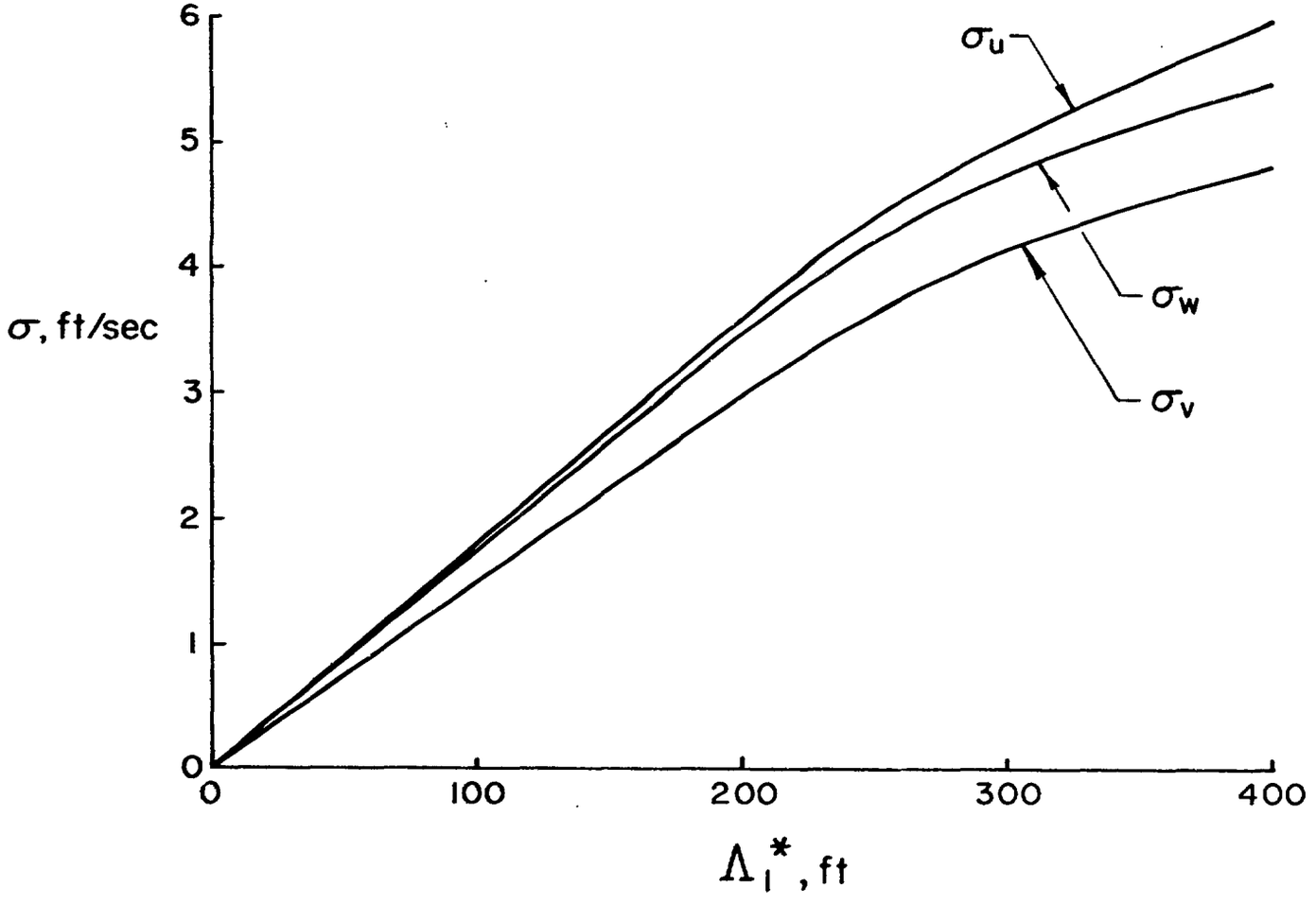

Fig. 26. Calculated turbulent intensities at an altitude of 750 ft as a function of the scale Λ_1^*

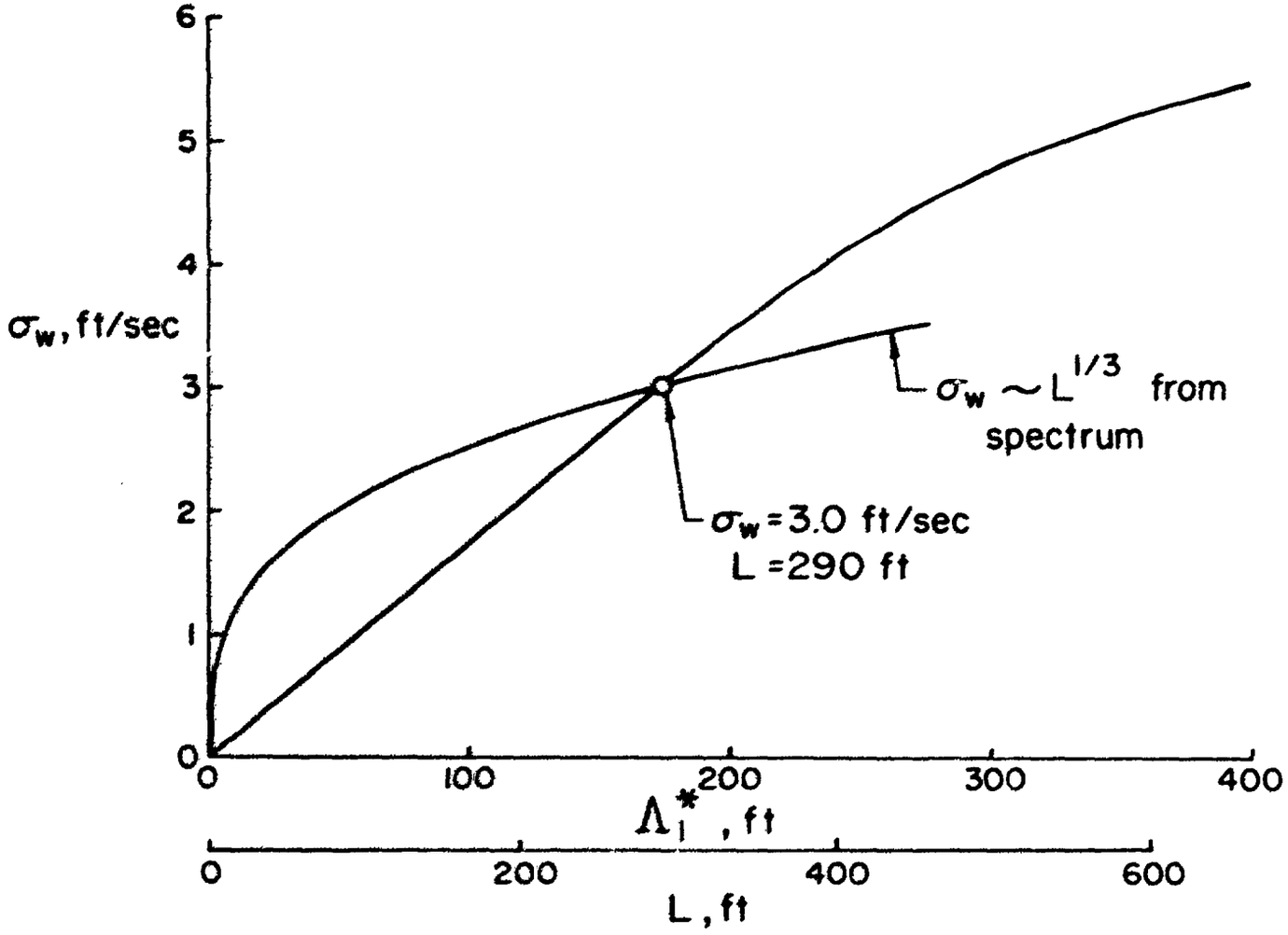

Fig. 27. Calculated turbulent intensity, σ_w, as a function of L compared with the relationship derived from the spectrum according to Eq. (5)

VII. DISCUSSION AND CONCLUSIONS

We have in this report presented a method for calculating turbulent shear flows that depends on the closure of the equations of motion at the second-order correlations of fluctuating quantities. This closure is accomplished by modeling the appropriate terms in the equations for the second-order correlations in terms of simple invariant expressions involving the second-order correlations themselves and several scale parameters. By comparison of computations with experiment, the relationships between the various scales were determined and the relationship of these scales to the integral scale in the turbulent flow that was being calculated was found. It was found that the basic scale Λ_1 used in the computation was approximately equal to three-fifths of the longitudinal integral scale of the turbulence under consideration.

Although it should be pointed out that more computations must be made before a final choice of model and model parameters is made, it is clear that some of the inconsistencies in the presently available experimental data on free turbulent shear layers should be cleared up first.

Once a turbulence model had been established and a relationship found between the computational scale used and the integral scale of the turbulent motion under consideration, the method was applied to the problem of obtaining, from partial atmospheric spectra, an estimate of the total turbulent intensities and the integral scales. By applying the method to a case of low altitude turbulence where the spectrum was complete enough to determine both the intensity and scale of turbulence but treating the spectrum as if it were incomplete, it was found that the magnitude of the turbulent intensity and scale could be evaluated if the mean wind and temperature profiles were known.

Although the method appears to work well, further studies of this type should be performed. At the present time, it is felt that the technique that has been developed is of sufficient interest to warrant support for these additional studies. An important part of these studies would be an application of the method to high altitude turbulence where the magnitude of the integral scale is not known.

In connection with such studies of high altitude turbulence, it is strongly recommended that all possible effort be expended to obtain mean atmospheric wind and temperature data as close in space and time to the actual measurement of turbulence as is possible.

APPENDIX A. CONSTANT DENSITY MODEL EQUATIONS FOR STEADY FLOW

Continuity:

$$\bar{u}^j{}_{,j} = 0 \tag{A.1}$$

Momentum:

$$\bar{u}^j \bar{u}_{i,j} = -\frac{1}{\rho}\bar{p}_{,i} + \nu\left(g^{jk}\bar{u}_{i,k}\right)_{,j} - \langle u^{j\prime} u_i' \rangle_{,j} \tag{A.2}$$

Stress tensor:

$$\begin{aligned}
\bar{u}^j \langle u_i' u_k' \rangle_{,j} = & -\langle u^{j\prime} u_k' \rangle \bar{u}_{i,j} - \langle u^{j\prime} u_i' \rangle \bar{u}_{k,j} \\
& + g^{j\ell}\left[\Lambda_2 q\left(\langle u_i' u_\ell' \rangle_{,k} + \langle u_\ell' u_k' \rangle_{,i} + \langle u_i' u_k' \rangle_{,\ell}\right)\right]_{,j} \\
& + \left[\Lambda_3 q \langle u^{\ell\prime} u_i' \rangle_{,\ell}\right]_{,k} + \left[\Lambda_3 q \langle u^{\ell\prime} u_k' \rangle_{,\ell}\right]_{,i} \\
& - \frac{q}{\Lambda_1}\left(\langle u_i' u_k' \rangle - g_{ik}\frac{K}{3}\right) + \nu\left[g^{j\ell}\langle u_i' u_k' \rangle_{,j\ell} - 2\frac{\langle u_i' u_k' \rangle}{\lambda^2}\right]
\end{aligned} \tag{A.3}$$

APPENDIX B. MODEL EQUATIONS FOR A BOUNDARY LAYER

We use a Cartesian coordinate system (x,y,z) with the free stream velocity in the x-direction and with a as the coordinate normal to the wall. The velocity components are denoted by (u,v,w). With the usual assumptions for a constant pressure boundary layer, Eqs. (A.1) through (A.3) become

$$\frac{\partial \bar{u}}{\partial x} + \frac{\partial \bar{w}}{\partial z} = 0 \tag{B.1}$$

$$\bar{u}\frac{\partial \bar{u}}{\partial x} + \bar{w}\frac{\partial \bar{u}}{\partial z} = \nu\frac{\partial^2 \bar{u}}{\partial z^2} - \frac{\partial \langle u'w' \rangle}{\partial z} \tag{B.2}$$

$$\bar{u}\frac{\partial \langle u'u' \rangle}{\partial x} + \bar{w}\frac{\partial \langle u'u' \rangle}{\partial z} = -2\langle u'w' \rangle \frac{\partial \bar{u}}{\partial z} + \frac{\partial}{\partial z}\left(\Lambda_2 q \frac{\partial \langle u'u' \rangle}{\partial z}\right) - \frac{q}{\Lambda_1}\left(\langle u'u' \rangle - \frac{K}{3}\right) + \nu\left(\frac{\partial^2 \langle u'u' \rangle}{\partial z^2} - \frac{2\langle u'u' \rangle}{\lambda^2}\right) \tag{B.3}$$

$$\bar{u}\frac{\partial \langle v'v' \rangle}{\partial x} + \bar{w}\frac{\partial \langle v'v' \rangle}{\partial z} = \frac{\partial}{\partial z}\left(\Lambda_2 q \frac{\partial \langle v'v' \rangle}{\partial z}\right) - \frac{q}{\Lambda_1}\left(\langle v'v' \rangle - \frac{K}{3}\right) + \nu\left(\frac{\partial^2 \langle v'v' \rangle}{\partial z^2} - \frac{2\langle v'v' \rangle}{\lambda^2}\right) \tag{B.4}$$

$$\bar{u}\frac{\partial \langle w'w' \rangle}{\partial x} + \bar{w}\frac{\partial \langle w'w' \rangle}{\partial z} = \frac{\partial}{\partial z}\left[(3\Lambda_2 + 2\Lambda_3)q \frac{\partial \langle w'w' \rangle}{\partial z}\right] - \frac{q}{\Lambda_1}\left(\langle w'w' \rangle - \frac{K}{3}\right) + \nu\left(\frac{\partial^2 \langle w'w' \rangle}{\partial z^2} - \frac{2\langle w'w' \rangle}{\lambda^2}\right) \tag{B.5}$$

$$\bar{u}\frac{\partial \langle u'w' \rangle}{\partial x} + \bar{w}\frac{\partial \langle u'w' \rangle}{\partial z} = -\langle w'w' \rangle \frac{\partial \bar{u}}{\partial z} + \frac{\partial}{\partial z}\left[(2\Lambda_2 + \Lambda_3)q \frac{\partial \langle u'w' \rangle}{\partial z}\right] - \frac{q}{\Lambda_1}\langle u'w' \rangle + \nu\left(\frac{\partial^2 \langle u'w' \rangle}{\partial z^2} - \frac{2\langle u'w' \rangle}{\lambda^2}\right) \tag{B.6}$$

APPENDIX C. MODEL EQUATIONS FOR A FREE JET

We use the cylindrical coordinate system (r,θ,z) with the velocity components denoted by (u,v,w), respectively. The assumptions for a constant pressure boundary layer are again applied to Eqs. (A.1) through (A.3), along with the assumption of axial symmetry, giving

$$\frac{\partial \bar{u}}{\partial r} + \frac{\bar{u}}{r} + \frac{\partial \bar{w}}{\partial z} = 0 \tag{C.1}$$

$$\bar{u}\frac{\partial \bar{w}}{\partial r} + \bar{w}\frac{\partial \bar{w}}{\partial z} = \nu\left(\frac{\partial^2 \bar{w}}{\partial r^2} + \frac{1}{r}\frac{\partial \bar{w}}{\partial r}\right) - \frac{\partial \langle u'w' \rangle}{\partial r} - \frac{\langle u'w' \rangle}{r} \tag{C.2}$$

$$\begin{aligned}
\bar{u}\frac{\partial \langle u'u' \rangle}{\partial r} + \bar{w}\frac{\partial \langle u'u' \rangle}{\partial z} &= \frac{\partial}{\partial r}\left[(3\Lambda_2 + 2\Lambda_3)q\frac{\partial \langle u'u' \rangle}{\partial r}\right] \\
&+ \frac{\Lambda_2 q}{r}\left(3\frac{\partial \langle u'u' \rangle}{\partial r} - 2\frac{\partial \langle v'v' \rangle}{\partial r}\right) \\
&+ \frac{2}{r}\frac{\partial}{\partial r}\left[\Lambda_3 q(\langle u'u' \rangle - \langle v'v' \rangle)\right] \\
&- \frac{(4\Lambda_2 + 2\Lambda_3)q}{r^2}(\langle u'u' \rangle - \langle v'v' \rangle) \\
&- \frac{q}{\Lambda_1}\left(\langle u'u' \rangle - \frac{K}{3}\right) + \nu\left[\frac{\partial^2 \langle u'u' \rangle}{\partial r^2} + \frac{1}{r}\frac{\partial \langle u'u' \rangle}{\partial r}\right. \\
&\left. - \frac{2}{r^2}(\langle u'u' \rangle - \langle v'v' \rangle) - \frac{2\langle u'u' \rangle}{\lambda^2}\right]
\end{aligned} \tag{C.3}$$

$$\bar{u}\frac{\partial\langle v'v'\rangle}{\partial r} + \bar{w}\frac{\partial\langle v'v'\rangle}{\partial z} = \frac{\partial}{\partial r}\left(\Lambda_2 q \frac{\partial\langle v'v'\rangle}{\partial r}\right) + \frac{3\Lambda_2 q}{r}\frac{\partial\langle v'v'\rangle}{\partial r}$$

$$+ \frac{2}{r}\frac{\partial}{\partial r}\left[\Lambda_2 q(\langle u'u'\rangle - \langle v'v'\rangle)\right] + \frac{2\Lambda_3 q}{r}\frac{\partial\langle u'u'\rangle}{\partial r}$$

$$+ \frac{(4\Lambda_2 + 2\Lambda_3)q}{r^2}(\langle u'u'\rangle - \langle v'v'\rangle)$$

$$- \frac{q}{\Lambda_1}\left(\langle v'v'\rangle - \frac{K}{3}\right) + \nu\left[\frac{\partial^2\langle v'v'\rangle}{\partial r^2} + \frac{1}{r}\frac{\partial\langle v'v'\rangle}{\partial r}\right.$$

$$\left. + \frac{2}{r^2}(\langle u'u'\rangle - \langle v'v'\rangle) - \frac{2\langle v'v'\rangle}{\lambda^2}\right] \qquad (C.4)$$

$$\bar{u}\frac{\partial\langle w'w'\rangle}{\partial r} + \bar{w}\frac{\partial\langle w'w'\rangle}{\partial z} = -2\langle u'w'\rangle\frac{\partial\bar{w}}{\partial r} + \frac{\partial}{\partial r}\left(\Lambda_2 q \frac{\partial\langle w'w'\rangle}{\partial r}\right) + \frac{\Lambda_2 q}{r}\frac{\partial\langle w'w'\rangle}{\partial r}$$

$$- \frac{q}{\Lambda_1}\left(\langle w'w'\rangle - \frac{K}{3}\right)$$

$$+ \nu\left(\frac{\partial^2\langle w'w'\rangle}{\partial r^2} + \frac{1}{r}\frac{\partial\langle w'w'\rangle}{\partial r} - \frac{2\langle w'w'\rangle}{\lambda^2}\right) \qquad (C.5)$$

$$\bar{u}\frac{\partial\langle u'w'\rangle}{\partial r} + \bar{w}\frac{\partial\langle u'w'\rangle}{\partial z} = -\langle u'u'\rangle\frac{\partial\bar{w}}{\partial r} + \frac{\partial}{\partial r}\left[(2\Lambda_2 + \Lambda_3)q\frac{\partial\langle u'w'\rangle}{\partial r}\right]$$

$$+ \frac{2\Lambda_2 q}{r}\frac{\partial\langle u'w'\rangle}{\partial r} + \frac{1}{r}\frac{\partial}{\partial r}\left[\Lambda_3 q\langle u'w'\rangle\right]$$

$$- \frac{(2\Lambda_2 + \Lambda_3)q}{r^2}\langle u'w'\rangle - \frac{q}{\Lambda_1}\langle u'w'\rangle$$

$$+ \nu\left(\frac{\partial^2\langle u'w'\rangle}{\partial r^2} + \frac{1}{r}\frac{\partial\langle u'w'\rangle}{\partial r} - \frac{\langle u'w'\rangle}{r^2} - \frac{2\langle u'w'\rangle}{\lambda^2}\right)$$

(C.6)

APPENDIX D. MODEL EQUATIONS FOR CLEAR AIR TURBULENCE

As in Ref. 2, we simplify the problem somewhat by assuming the mean flow is in the x direction only and that all the dependent variables are functions only of time t and altitude z. The convective operators in the steady state equations $u^j(\partial/\partial x_j)$ are replaced by $\partial/\partial t$.

In considering atmospheric motions, we include buoyancy terms and temperature terms that induce them. We take the actual mean temperature to be the sum of an adiabatic temperature $T_o(z)$ and a departure therefrom denoted $\bar{T}(z,t)$. The density corresponding to the adiabatic temperature variation is denoted by $\rho_o(z)$ and we write

$$\sigma = \frac{1}{\rho_o}\frac{\partial \rho_o}{\partial z}$$

The equations before modeling are given in Ref. 2. With the current modeling, they become

$$\rho_o \frac{\partial \bar{u}}{\partial t} = \mu \frac{\partial^2 \bar{u}}{\partial z^2} - \frac{\partial(\rho_o \langle u'w' \rangle)}{\partial z} \tag{D.1}$$

$$\rho_o \frac{\partial \bar{T}}{\partial t} = \mu \frac{\partial^2 \bar{T}}{\partial z^2} - \frac{\partial(\rho_o \langle w'T' \rangle)}{\partial z} \tag{D.2}$$

$$\rho_o \frac{\partial \langle u'u' \rangle}{\partial t} = -2\rho_o \langle u'w' \rangle \frac{\partial \bar{u}}{\partial z} + \frac{\partial}{\partial z}\left(\rho_o \Lambda_2 q \frac{\partial \langle u'u' \rangle}{\partial z}\right)$$
$$- \frac{\rho_o q}{\Lambda_1}\left(\langle u'u' \rangle - \frac{K}{3}\right) + \mu\left(\frac{\partial^2 \langle u'u' \rangle}{\partial z^2} - \frac{2\langle u'u' \rangle}{\lambda^2}\right) \tag{D.3}$$

$$\rho_o \frac{\partial \langle v'v' \rangle}{\partial t} = \frac{\partial}{\partial z}\left(\rho_o \Lambda_2 q \frac{\partial \langle v'v' \rangle}{\partial z}\right) - \frac{\rho_o q}{\Lambda_1}\left(\langle v'v' \rangle - \frac{K}{3}\right)$$
$$+ \mu\left(\frac{\partial^2 \langle v'v' \rangle}{\partial z^2} - \frac{2\langle v'v' \rangle}{\lambda^2}\right) \tag{D.4}$$

$$\rho_o \frac{\partial \langle w'w' \rangle}{\partial t} = \frac{\partial}{\partial z}\left[\rho_o(3\Lambda_2 + 2\Lambda_3)\, q \frac{\partial \langle w'w' \rangle}{\partial z}\right] + 2\frac{\partial \rho_o}{\partial z}\Lambda_3 q \frac{\partial \langle w'w' \rangle}{\partial z}$$
$$- \frac{\rho_o q}{\Lambda_1}\left(\langle w'w' \rangle - \frac{K}{3}\right) + \mu\left(\frac{\partial^2 \langle w'w' \rangle}{\partial z^2} - \frac{2\langle w'w' \rangle}{\lambda^2}\right)$$
$$- 2(\mu + \mu^*)\left(\frac{\partial \sigma}{\partial z} - \sigma^2\right)\langle w'w' \rangle + \frac{2\rho_o g}{T_o}\langle w'T' \rangle \tag{D.5}$$

$$\rho_o \frac{\partial \langle u'w' \rangle}{\partial t} = - \rho_o \langle w'w' \rangle \frac{\partial \bar{u}}{\partial z} + \frac{\partial}{\partial z} \left[\rho_o (2\Lambda_2 + \Lambda_3) q \frac{\partial \langle u'w' \rangle}{\partial z} \right]$$

$$+ \frac{\partial \rho_o}{\partial z} \Lambda_3 q \frac{\partial \langle u'w' \rangle}{\partial z} - \frac{\rho_o q}{\Lambda_1} \langle u'w' \rangle$$

$$+ \mu \left[\frac{\partial^2 \langle u'w' \rangle}{\partial z^2} - \frac{2 \langle u'w' \rangle}{\lambda^2} \right] - (\mu + \mu^*) \left(\frac{\partial \sigma}{\partial z} - \sigma^2 \right) \langle u'w' \rangle$$

$$+ \frac{\rho_o g}{T_o} \langle u'T' \rangle \qquad \text{(D.6)}$$

$$\rho_o \frac{\partial \langle u'T' \rangle}{\partial t} = - \rho_o \langle u'w' \rangle \frac{\partial \bar{T}}{\partial z} - \rho_o \langle w'T' \rangle \frac{\partial \bar{u}}{\partial z} + \frac{\partial}{\partial z} \left(\rho_o \Lambda_2 q \frac{\partial \langle u'T' \rangle}{\partial z} \right)$$

$$- \frac{\rho_o q}{\Lambda_1} \langle u'T' \rangle + \mu \left(\frac{\partial^2 \langle u'T' \rangle}{\partial z^2} - \frac{2 \langle u'T' \rangle}{\lambda^2} \right) \qquad \text{(D.7)}$$

$$\rho_o \frac{\partial \langle w'T' \rangle}{\partial t} = - \rho_o \langle w'w' \rangle \frac{\partial \bar{T}}{\partial z} + \frac{\partial}{\partial z} \left[\rho_o (2\Lambda_2 + \Lambda_3) q \frac{\partial \langle w'T' \rangle}{\partial z} \right]$$

$$- \frac{\rho_o q}{\Lambda_1} \langle w'T' \rangle + \mu \left(\frac{\partial^2 \langle w'T' \rangle}{\partial z^2} - \frac{2 \langle w'T' \rangle}{\lambda^2} \right)$$

$$- (\mu + \mu^*) \left(\frac{\partial \sigma}{\partial z} - \sigma^2 \right) \langle w'T' \rangle + \frac{\rho_o g}{T_o} \langle T'T' \rangle \qquad \text{(D.8)}$$

$$\rho_o \frac{\partial \langle T'T' \rangle}{\partial t} = - 2\rho_o \langle w'T' \rangle \frac{\partial \bar{T}}{\partial z} + \frac{\partial}{\partial z} \left(\rho_o \Lambda_2 q \frac{\partial \langle T'T' \rangle}{\partial z} \right)$$

$$+ \mu \left(\frac{\partial^2 \langle T'T' \rangle}{\partial z^2} - \frac{2 \langle T'T' \rangle}{\lambda^2} \right) \qquad \text{(D.9)}$$

In these equations, μ^* is the second coefficient of viscosity and g is the acceleration of gravity.

REFERENCES

1. Donaldson, Coleman duP. and Rosenbaum, Harold, "Calculation of Turbulent Shear Flows Through Closure of the Reynolds Equations by Invariant Modeling," A.R.A.P. Report No. 127, December 1968. Also published in Proceedings of Symposium on Compressible Turbulent Boundary Layers, NASA SP-216, pp. 231-253.

2. Donaldson, Coleman duP., Sullivan, Roger D., and Rosenbaum, Harold, "Theoretical Study of the Generation of Atmospheric Clear Air Turbulence," AIAA Paper No. 70-55, New York, January 1970 (to be published in AIAA Journal).

3. Hinze, J.O., Turbulence, McGraw Hill, New York, 1959, p. 172.

4. Houbolt, John C., Steiner, Roy, and Pratt, Kermit G., "Dynamic Response of Airplanes to Atmospheric Turbulence Including Flight Data on Input and Response," NASA TR R-199, June 1964.

5. Reynolds, Osborne, "On the Dynamical Theory of Incompressible Viscous Fluids and the Determination of the Criterion," Phil. Trans. Royal Society, London, A 186, 1894, p. 123.

6. Rotta, J., "Statistische Theorie nichthomogener Turbulenz," Z. Physik, Vol. 129, 1951, p. 547.

7. Chou, P.Y., "Pressure Flow of a Turbulent Fluid between Two Infinite Parallel Planes," Quart. Applied Math, Vol. 3, No. 3, 1949, pp. 198-209.

8. Hanjalic, K. and Launder, B.E., "A Reynolds Stress Model of Turbulence and its Application to Asymmetric Boundary Layers," Imp. College of Science & Technology, London, Report No. TM/TN/A/8, March 1971.

9. Donaldson, Coleman duP., "Calculation of Turbulent Shear Flows for Atmospheric and Vortex Motions," AIAA Paper No. 71-217, New York, January 1971 (to be published in AIAA Journal).

10. Donaldson, Coleman duP. and Conrad, Peter W., "Computations of the Generation of Turbulence in the Atmospheric Boundary Layer," Proceedings of the International Conference on Atmospheric Turbulence, London, The Royal Aeronautical Society, May 1971.

11. Wygnanski, I. and Fiedler, H., "Some Measurements in the Self-Preserving Jet," J. Fluid Mech., Vol. 38, Part 3, 1969, pp. 577-612.

12. Wygnanski, I. and Fiedler, H., "The Two-Dimensional Mixing Region," J. Fluid Mech., Vol. [illegible], 1971, pp. 327-361.

13. Gibson, M.M., "Spectra of Turbulence in a Round Jet," J. Fluid Mech., Vol. 15, Part 2, 1963, pp. 161-173.

14. Donaldson, Coleman duP., Snedeker, Richard S. and Margolis, David P., "A Study of Free Jet Impingement. Part 2. Free Jet Turbulent Structure and Impingement Heat Transfer," J. Fluid Mech., Vol. 45, Part 3, 1971, pp. 477-512.

15. Tollmien, W., "Berechnung turbulenter Ausbreitungsvorgange," Zeitschrift für angewandte Mathematik und Mechanik, Vol. IV, 1926, p. 468.

16. Prandtl, L., "The Mechanics of Viscous Fluids," Aerodynamic Theory (W. Durand, editor), Stanford University Press, 1934, pp. 34-208.

17. Prandtl, L. and Wieghardt, K., "Uber ein neues Formelsystem fur die ausgebildte Turbulenz," Nachr. Akad. Wiss. Goettingen, 19, 6, 1945.

18. Glushko, G.S., Turbulent Boundary Layer on a Flat Plate in an Incompressible Fluid," Bull. Acad. Science USSR, Mech. Series No. 4, 1965, pp. 13-23.

19. Bradshaw, P., Ferriss, D.H., and Atwell, N.P., "Calculations of Boundary Layer Development Using the Turbulent Energy Equation," J. Fluid Mech., Vol. 28, Part 3, 1967, pp. 593-616.

20. Harlow, F.H. and Romero, N.C., "Turbulence Distortion in a Nonuniform Tunnel," LASL Report No. LA-4247, 1969.

21. Jawain, T.H. and Pritchett, J.W., "A Unified Heuristic Model of Fluid Turbulence," J. Comp. Physics, Vol. 5, No. 3, 1970, pp. 383-405.

22. Beckwith, I.E. and Bushnell, D.M., "Detailed Description and Results of a Method for Computing Mean and Fluctuating Quantities in Turbulent Boundary Layers, NASA TN-D-4815, 1968.

23. Coles, Donald, "Measurements in the Boundary Layer on a Smooth Flat Plate in Supersonic Flow. Part I. The Problem of the Turbulent Boundary Layer, "JPL Report No. 20-69, 1953.

24. Grant, H.L., "The Large Eddies of Turbulent Motion," J. Fluid Mech., Vol. 4, Part 2, 1958, pp. 149-190.

25. Jones, J.W., Mielke, R.R., and Jones, J.W., et al., "Low Altitude Atmospheric Turbulence. LO-LOCAT Phase III. Vol. II, Part II Frequency Data Plots," AFFDL-TR-70-10, Vol. II, Part II, November 1970.

26. _____ "... Vol. II, Part I Data Acquisition and Processing. Data Plots, and Tabulations," AFFDL-TR-70-10, Vol. II, Part I, November 1970.

27. Monson, K.R., Jones, G.W., and Mielke, R.H., et al., "Low Altitude Atmospheric Turbulence, LO-LOCAT Phase III Interim Report," ASD-TR, May 1969.